In vivo and cellular antiarrhythmic and cardiac electrophysiological effects of desethylamiodarone in dog cardiac preparations

Running title: Cardiac electrophysiological effects of desethylamiodarone

Zsófia Kohajda[2,*], László Virág[1,3,*], Tibor Hornyik[1], Zoltán Husti[1], Anita Sztojkov-Ivanov[4], Norbert Nagy[1,2], András Horváth[1], Richárd Varga[1], János Prorok[1,2], Jozefina Szlovák[1], Noémi Tóth[1], Péter Gazdag[1], Leila Topal[1], Muhammad Naveed[1], Tamás Árpádffy-Lovas[1], Bence Pászti[1], Tibor Magyar[1], István Koncz[1], Szilvia Déri[1], Vivien Demeter-Haludka[1], Zoltán Aigner[5], Balázs Ördög[1], Márta Patfalusi[6], László Tálosi[7], László Tiszlavicz[8], Imre Földesi[9], Norbert Jost[1,2,3], István Baczkó[1,3,*], András Varró[1,2,3,*,#]

[1] Department of Pharmacology and Pharmacotherapy, University of Szeged, Szeged, Hungary

[2] ELKH-SZTE Research Group for Cardiovascular Pharmacology, Eötvös Loránd Research Network, Szeged, Hungary

[3] Department of Pharmacology and Pharmacotherapy, Interdisciplinary Excellence Centre, University of Szeged, Szeged, Hungary

[4] Department of Pharmacodynamics and Biopharmacy, University of Szeged, Szeged, Hungary.

[5] Institute of Pharmaceutical Technology and Regulatory Affairs, University of Szeged, Szeged, Hungary

[6] ATRC Aurigon Toxicological Research Center Ltd., Dunakeszi, Hungary

[7] Department of Pharmacognosy, Faculty of Pharmacy, University of Szeged, Szeged, Hungary.

[8] Department of Pathology, Faculty of Medicine, University of Szeged, Szeged, Hungary.

[9] Department of Laboratory Medicine, Faculty of Medicine, University of Szeged, Szeged, Hungary

Corresponding author: András Varró, E-mail: varro.andras@med.u-szeged.hu

This article has been accepted for publication and undergone full peer review but has not been through the copyediting, typesetting, pagination and proofreading process which may lead to differences between this version and the Version of Record. Please cite this article as doi: 10.1111/bph.15812

* Shared first and senior authorship

Data availability statement:

The data that support the findings of this study are available from the corresponding author upon reasonable request.

ABSTRACT

Background and Purpose: The aim of the present study was to study the antiarrhythmic effects and cellular mechanisms of desethylamiodarone (DEA), the main metabolite of amiodarone (AMIO), following acute and chronic 4-week oral treatments (25-50 mg kg^{-1} day^{-1}).

Experimental Approach and Key Results: Acute iv. (10 mg kg^{-1}) and chronic oral (4 weeks, 25 mg $kg^{-1}day^{-1}$) administrations of DEA exerted marked antiarrhythmic effects in carbachol and tachypacing induced dog atrial fibrillation models, respectively. Both acute (10 μM) and chronic (p.o. 4 weeks, 50 mg kg^{-1} day^{-1}) DEA administration prolonged action potential duration in atrial and ventricular muscle without changing it in Purkinje fiber measured by the conventional microelectrode technique. DEA decreased the amplitude of several outward potassium currents such as I_{Kr}, I_{Ks}, I_{K1}, I_{to} and I_{KACh} measured by the whole cell configuration of the patch-clamp technique. The L-type I_{Ca} and late I_{Na} inward currents were also significantly depressed by acute DEA treatment. Pharmacokinetic studies following a single intravenous dose of 25 mg kg^{-1} revealed better drug bioavailability and higher volume of distribution with DEA than with AMIO. Chronic toxicological investigations (91 days) with DEA showed no neutropenia and less severe pulmonary fibrosis compared to that of AMIO treatment.

Conclusion and Implications: Chronic DEA treatment in animal experiments has marked antiarrhythmic and electrophysiological effects with better pharmacokinetics and lower toxicity than its parent compound. These results suggest that the active metabolite, DEA

should be considered to be tested in clinical trials as a possible new, more favorable option for the treatment of cardiac arrhythmias including atrial fibrillation.

Key words: desethylamiodarone, atrial fibrillation, cardiac electrophysiology, canine

Abbreviations: ACTB, ß-actin; AERP, atrial effective refractory period; AF, atrial fibrillation; AMIO, amiodarone; APA, action potential amplitude; APD, action potential duration; APD_{50}, APD_{90}, action potential duration measured at 50% and 90% repolarization; APD_{SS}, maximal action potential duration; AUC_{inf}, area under the plasma concentration-time curve extrapolated to infinity; $AUC_{intravenous}$, area under the plasma concentration-time curve following intravenous administration; AUC_{last}, area under the plasma concentration-time curve from time zero to last measurable concentration; AUC_{oral}, area under the plasma concentration-time curve following oral administration; AV, atrioventricular; B2M, ß2-microglobulin; BCL, basic cycle length; Cl, clearance; C_{max}, measured peak concentration; DAD, delayed afterdepolarization; DEA, desethylamiodarone; F, bioavailability; HPLC, high-performance liquid chromatography; HPRT, hypoxanthine phosphoribosyltransferase; I_{CaL}, L-type calcium current; I_{K1}, inward rectifier potassium current; I_{KACh}, acetylcholine activated potassium current; I_{Kr}, rapid delayed rectifier potassium current; I_{Ks}, slow delayed rectifier potassium current; I_{Naf}, fast sodium current; I_{NaL}, late sodium current; I_{to}, transient outward potassium current; qRT-PCR, quantitative real-time reverse transcription polymerase chain reaction; QTc, frequency-corrected QT interval; RP, resting potential; RPS5, 40S ribosomal protein S5; SRP14, signal recognition particle 14; T_{lag}, absorption lag time; T_{max}, time of peak concentration; TTX, tetrodotoxin; V_{max}, maximum upstroke velocity; V_{SS}, volume of distribution at steady state; VVI mode, ventricular sensing, pacing and pacing output in response to a sensed ventricular event is inhibited

What is already known

- Desethylamiodarone is the main metabolite of amiodarone, the most prescribed and most powerful antiarrhythmic drug.
- Acute desethylamiodarone reduces experimental ventricular arrhythmias and its acute cardiac electrophysiological effects have been described.

What this study adds

- Chronic desethylamiodarone administration exhibits similar electrophysiological and atrial antiarrhythmic effects to those reported for amiodarone.
- More favourable hematological, pulmonary toxicity and pharmacokinetic properties are observed with desethylamiodarone compared to amiodarone.

What is the clinical significance

- These results suggest that desethylamiodarone should be studied in the clinical setting for arrhythmia management.

INTRODUCTION

Ventricular arrhythmias, which may degenerate into ventricular fibrillation and lead to sudden cardiac death, cause the worldwide loss of approximately 18 million lives each year (Shomanova et al., 2020). In addition, the most common sustained arrhythmia, atrial fibrillation (AF) is a major health burden in developed countries (Kavousi et al., 2020). AF significantly increases cardiovascular mortality by eliciting stroke and ventricular arrhythmias. Although current antiarrhythmic therapies do not decrease AF related mortality, further advances in antiarrhythmic drug therapy is needed to improve quality of life and life expectancy in large number of patients suffering from AF.

It is generally accepted that AMIO is the most powerful drug to treat arrhythmias including AF (Kudenchuk et al., 1999; Mujović et al., 2020). However, long-term treatment with AMIO leads to significant tissue accumulation and serious organ toxicity related adverse effects which greatly limit its widespread use (Kudenchuk et al., 1999). During chronic AMIO treatment, an active metabolite, desethylamiodarone (DEA) appears in the plasma and accumulates in different organs (Adams et al., 1985; Kodama et al., 1999) including the heart. In some animal studies, acute application of DEA produced pharmacological and electrophysiological effects similar to those following AMIO administration (Talajic et al., 1987; Nattel et al., 1988).

In spite of the abundant evidence that DEA appears in the plasma and accumulates in the cardiac tissue (Adams et al., 1985) reaching even higher concentrations than its parent drug AMIO, there are very few data regarding the cardiac electrophysiological and antiarrhythmic effects of chronic oral DEA treatment. This is especially true for large animal models which have more translational value than results obtained in small rodents. Results are entirely lacking about the effects of DEA on experimental atrial fibrillation, and in large animals in the normal heart, especially following long-term administration.

Therefore, the aim of the present study was to thoroughly investigate the acute and chronic cardiac electrophysiological effects of DEA and its impact on atrial fibrillation in a large animal model and in preparations isolated from these animals.

METHODS

Animals and materials

All experiments were carried out in compliance with the Guide for the Care and Use of Laboratory Animals (USA NIH publication NO 85-23, revised 1996) and conformed to the Directive 2010/63/EU of the European Parliament. The protocols have been approved by the Ethical Committee for the Protection of Animals in Research of the University of Szeged,

Szeged, Hungary (approval numbers: I-74-15-2017 and I-74-24-2017) and by the Department of Animal Health and Food Control of the Ministry of Agriculture and Rural Development (authority approval numbers XIII/3330/2017 and XIII/3331/2017). Animal housing and handling was in accordance with good animal practice as defined by the Federation of European Laboratory Animal Science Association, FELASA. Animal studies were reported in compliance with the ARRIVE guidelines (Kilkenny et al., 2010) and with the editorial on reporting animal studies (McGrath et al., 2015). Dogs were housed in dog-kennels that fulfilled the legal requirements in terms of size and environmental enrichment, including elevated resting places for each dog. The animals were kept at standard room temperature, humidity and lighting. Food was provided twice a day and drinking water was given *ad libitum*.

In order to study the electrophysiological effects of DEA, adult Beagle dogs (age: 14-26 months, purchased from a certified experimental animal breeder, Ásotthalom, Hungary; breeder authority approval number: XXXV/2018 by the Department of Animal Health and Food Control of the Ministry of Agriculture and Rural Development, Hungary) of either sex weighing 12–15 kg (n=38) were treated with DEA (1x25 mg kg^{-1} day^{-1} or 2x25 mg kg^{-1} day^{-1}, per os) for 4 weeks. For comparison, 30 untreated dogs were used (Control group). In order to compare the plasma levels and tissue concentrations, another 27 adult Beagle dogs of either sex were treated with AMIO (2x25 mg kg^{-1} day^{-1}, per os) for 4 weeks. Another 7 male Beagle dogs were used for the chronic atrial tachypacing-induced AF conscious dog experiments. In the acute carbachol induced canine AF model measurements, 12 adult Beagle dogs of either sex (control group: n=6; DEA group: n=6) were used. For exploratory, non-GLP chronic toxicological investigations in large animals, 4 – 4 Beagle dogs of either sex were orally treated with DEA or AMIO (25 mg kg^{-1} day^{-1}) for 91 days. The details of general anesthesia are described in the appropriate subsections.

All materials except collagenase (Worthington Biochemical Corp., Lakewood, NJ, USA), TTX (Bio-Techne R&D Systems Ltd. – Tocris, Budapest, Hungary), and AMIO (Sequoia Research Products Ltd., Pangbourne, UK) purchased from Sigma-Aldrich Ltd. (Budapest, Hungary). DEA was synthetized by order and purchased from ChemEast Laboratory Ltd. Budapest, Hungary.

Chronic atrial tachypacing induced AF in conscious dogs

Male Beagle dogs (n=7) weighing 12-15 kg were used for the experiments. The dogs were accommodated to experimental personnel and equipment, every day for a week before the start of the studies. The pacemaker and pacemaker electrode implantation procedures were performed under ketamine (Richter Gedeon Ltd., Hungary; induction: 10 mg kg^{-1} i.v., maintenance: 2 mg kg^{-1}, every 20 min) + xylazine (CP-Pharma Handelsges, Germany; induction: 1 mg kg^{-1}, maintenance: 0.2 mg kg^{-1}, every 20 min) anesthesia as described previously (Baczko et al., 2014). For antibiotic coverage, amoxicillin/clavulanic acid (1000 mg/200 mg i.v.; Richter Gedeon Ltd.) and gentamicin (40 mg i.v.; Sandoz GmbH, Kundl, Austria) were given before the operation, and amoxicillin/clavulanic acid 500 mg/125 mg (Augmentin 500mg/125mg®; GlaxoSmithKline Ltd., Hungary) orally, twice a day for 5 days was given following the operation. For peri-operative analgesia metamizole sodium (1000 mg i.v., 1g $2ml^{-1}$; Sanofi-Aventis Hungary Ltd., Hungary) and tramadol (50 mg i.v., TEVA Ltd., Hungary, under licence from Grünenthal GmbH, Aachen, Germany) were administered. Briefly, two bipolar pacemaker electrodes (Synox SX 53-JBP and Synox SX 60/15-BP, Biotronik Hungary Ltd., Hungary) were positioned into the right atrial appendage and apex of the right ventricle, respectively, and the electrodes were connected to pacemakers (Logos DS and Philos S, Biotronik Hungary Ltd., Hungary) in subcutaneous pockets in the neck area, followed by radiofrequency catheter ablation of the AV node. The pacemakers were

programmed by the ICS 3000 Programmer (Biotronik Hungary Ltd., Hungary). Following recovery from surgery (3-5 days), right atrial tachypacing was started at 400 beats min^{-1} (at twice threshold, with a 0.4 ms pulse width), maintained for 6 to 7 weeks before the experiments to allow electrical remodeling of the atria (monitored by the measurement of the right atrial effective refractory period (AERP) every second day). The AERPs were measured at basic cycle lengths (BCL) of 150 and 300 ms with a train of 10 stimuli (S1) followed by an extra stimulus (S2), with the AERP defined as the longest S1-S2 interval that did not produce a response. The S2 stimulus was gradually decreased from 150 ms in 10 ms steps during the measurements. The AERP measurement did not evoke atrial fibrillation in any of the animals. Due to pacemaker manufacturing specifications (the lower adjustable limit for the S1-S2 intervals was 80 ms), AERP shorter than 80 ms could not be measured in our conscious animals.

On the day of the experiment atrial pacing was stopped, continuous recording of the electrocardiogram started using precordial leads and the AERP was measured. A control set (25 times) of 10-second-long rapid atrial bursts (800 beats min^{-1}, at twice threshold) were performed in order to induce atrial fibrillation in conscious dogs. The ECG was recorded using precordial leads, was digitized and stored on a computer for off-line analysis using National Instruments data acquisition hardware (National Instruments, Austin, Texas, USA) and SPEL Advanced Haemosys software (version 3.2, MDE Heidelberg GmbH, Heidelberg, Germany). The incidence of AF, the total duration of AF, the average duration of AF episodes was measured and calculated along with changes in AERP and QT interval. QT intervals were measured on dogs with pacemaker implantation before the 12^{th} burst and were not corrected for heart rate since QT measurements were made at the heart rate set to 80 beats min^{-1} by the ventricular pacemaker. Experiments were performed in freely moving conscious dogs so that any effects of anesthetics on AERP and AF could be ruled out. After control

measurements animals were treated with 25 mg kg^{-1} DEA orally every day for 4 weeks and AF provocation repeated in each dog.

Acute carbachol induced canine AF model

Beagle dogs of either sex (control group: n=6; DEA group: n=6) weighing 12–14 kg were used for the experiments. Following 5 µg kg^{-1} intravenous sufentanyl (Sufentanil Torrex 5 µg ml^{-1}; Chiesi Pharmaceuticals GmbH, Vienna, Austria) premedication and 30 mg kg^{-1} intravenous pentobarbital sodium (Release 300 mg ml^{-1}; WDT, Garbsen, Germany) anesthesia induction, left thoracotomy was performed on all animals. Dogs were endotracheally intubated and mechanically ventilated (UGO Basile S.R.L. respirator; Biological Research Apparatus VA Italy). A continuous intravenous infusion of sufentanyl at a dose of 5 µg kg^{-1} h^{-1} and repeated intravenous administration of pentobarbital sodium at a dose of 15 mg kg^{-1} every 30 min were used to ensure adequate anesthesia depth during surgery and experiments. Physiological parameters (non-invasive blood pressure, SpO_2, ECG) were continuously monitored during surgery and experiments (InnoCare-VET Patient Care Monitor; Innomed Medical Inc., Budapest, Hungary). The ECG was recorded using precordial leads and was digitized and stored on a computer for off-line analysis using National Instruments data acquisition hardware (National Instruments, Austin, Texas, USA) and SPEL Advanced Haemosys software (version 3.2, MDE Heidelberg GmbH, Heidelberg, Germany). Two pacemaker electrodes (Biotronik Solia S 60; Biotronik Hungary Ltd., Hungary) were positioned epicardially into the left atrial appendage and apex of the left ventricle, respectively, and electrodes were connected to pacemakers (Effecta D; Biotronik Hungary Ltd., Hungary). Pacemakers were programmed in VVI mode using Biotronik ICS 3000 DS CD-W US programmer to prevent the potentially bradycardizing effect of carbachol leading to hemodynamic instability. Atrial and ventricular threshold were measured before

AF induction in all animals. Ventricular and atrial pacing were set to three times the measured threshold. AF inducibility were tested in both groups using a control set (25 times) of 10-second-long rapid atrial bursts (800 beats min^{-1}, at three times threshold). Following 25 atrial burst stimulus, 2x20 µg kg^{-1} loading dose of intravenous carbachol (Carbamylcholine chloride; Sigma-Aldrich) was administered followed by 80 µg kg^{-1} h^{-1} maintenance dose. Atrial fibrillation was induced using 10-second-long atrial burst stimulus in the presence of carbachol in both groups of dogs. Atrial fibrillation when evoked by carbachol infusion never converted spontaneously to sinus rhythm in the control group of dogs (n= 6). The DEA group of dogs (n= 6) received 10 mg kg^{-1} DEA (Szintekon Co, Ltd., Hungary; dissolved in Sulfobutylated beta-cyclodextrin sodium salt; CycloLab Cyclodextrin Research and Development Laboratory Ltd., Hungary) in 5 min. After conversion to sinus rhythm, inducibility of AF was repeatedly tested using 10-second-long atrial burst stimulus in the presence of carbachol (control group) and in the presence of carbachol and desethylamiodarone (DEA group). In the experiments, we investigated whether AF is converted to SR under the effect of DEA. All intravenous infusions were performed using a programmable infusion pump (Terufusion TE-3; Terumo Europe, Leuven, Belgium). At the end of the experiments, the animals received intravenous injection of 400 U/kg heparin and euthanasia was performed by i.v. administered pentobarbital sodium (30 mg kg^{-1}, i.v.).

Conventional microelectrode technique

Action potentials were recorded in atrial and right ventricular trabecular or papillary muscle and Purkinje fiber preparations obtained from dog hearts using conventional microelectrode techniques (Varró et al., 2001). Beagle dogs (either sex, 10–15 kg) were anesthetized with pentobarbital sodium (30 mg kg^{-1}, i.v.) following sedation (xylazine 1 mg kg^{-1}, i.v.). The animals also received intravenous injection of 400 U kg^{-1} heparin.

Preparations were individually mounted in a tissue chamber with a volume of 50 ml. During experiments modified Locke's solution was used, containing (in mM): NaCl 128.3, KCl 4, $CaCl_2$ 1.8, $MgCl_2$ 0.42, $NaHCO_3$ 21.4, and glucose 10. The pH of this solution was set between 7.35 and 7.4 when gassed with the mixture of 95% O_2 and 5% CO_2 at 37°C. Each preparation was stimulated through a pair of platinum electrodes in contact with the preparation using rectangular current pulses of 1-3 ms duration at twice of the threshold strength at a constant basic cycle length of 1000 ms for ventricular and 500 ms for atrial preparations (S1). These stimuli were delivered for at least 60 min allowing the preparation to equilibrate before the measurements were initiated. Transmembrane potentials were recorded using conventional glass microelectrodes, filled with 3 M KCl and having tip resistances of 5–20 MΩ, connected to the input of a high impedance electrometer (Experimetria, type 309, Budapest, Hungary) which was coupled to a dual beam oscilloscope.

The resting potential (RP), action potential amplitude (APA), maximum upstroke velocity (V_{max}), and APD measured at 50% and 90% of repolarization (APD_{50} and APD_{90}, respectively) were determined off-line using an in-house developed software (APES) running on a computer equipped with an ADA 3300 analog-to-digital data acquisition board (Real Time Devices, Inc., State College, Pennsylvania) having a maximum sampling frequency of 40 kHz.

The following types of stimulations were applied in the course of the experiments: stimulation with a constant cycle length of 1000 ms; stimulation with different constant cycle lengths ranging from 300 to 5000 ms. To determine the recovery kinetics of V_{max} and APD_{90} (APD_{90} restitution), extra test action potentials were elicited after every 20^{th} basic S1 beat by using single test pulses (S2) in a preparation driven at a basic cycle length of 400 and 1000 ms, respectively. The S1–S2 coupling interval was increased progressively from the end of the refractory period. The diastolic intervals preceding the test action potential were

measured from the point corresponding to 90% of repolarization of the preceding basic beat to the upstroke of the test action potential and were increased progressively. Onset kinetics was measured with a 400 ms cycle length train of stimuli after a 1-minute rest.

Attempts were made to maintain the same impalement throughout each experiment. In case an impalement became dislodged, adjustment was attempted, and if the action potential characteristics of the re-established impalement deviated by less than 5% from the previous measurement, the experiment continued.

Patch-clamp measurements

Beagle dogs (either sex, 10–15 kg) were anesthetized with pentobarbital sodium (30 mg kg^{-1}, i.v.) following sedation (xylazine 1 mg kg^{-1}, i.v.). The animals also received intravenous injection of 400 IU kg^{-1} heparin. Ventricular myocytes were enzymatically dissociated from canine hearts as described earlier in detail (Jost et al., 2013). One drop of cell suspension was placed in a transparent recording chamber mounted on the stage of an inverted microscope (Olympus IX51, Olympus, Tokyo, Japan), and individual myocytes were allowed to settle and adhere to the chamber bottom for at least 5-10 min before superfusion was initiated and maintained by gravity. Only rod-shaped cells with clear striations were used. HEPES-buffered Tyrode's solution (composition in mM: NaCl 144, NaH_2PO_4 0.4, KCl 4.0, $CaCl_2$ 1.8, $MgSO_4$ 0.53, glucose 5.5 and HEPES 5.0, at pH of 7.4) served as the normal superfusate.

Micropipettes were fabricated from borosilicate glass capillaries (Science Products GmbH, Hofheim, Germany), using a P-97 Flaming/Brown micropipette puller (Sutter Co, Novato, CA, USA), and had a resistance of 1.5-2.5 MOhm when filled with pipette solution. The membrane currents were recorded with Axopatch-200B amplifiers (Molecular Devices, Sunnyvale, CA, USA) by means of the whole-cell configuration of the patch-clamp

technique. The membrane currents were digitized with 250 kHz analogue to digital converters (Digidata 1440A, Molecular Devices, Sunnyvale, CA, USA) under software control (pClamp 10 (RRID:SCR_011323), Molecular Devices, Sunnyvale, CA, USA). Experiments were carried out at 37 °C.

Measurement of L-type calcium current

The L-type calcium current (I_{CaL}) was recorded in HEPES-buffered Tyrode's solution supplemented with 3 mM 4-aminopyridine. A special solution was used to fill the micropipettes (composition in mM: CsCl 125, TEACl 20, MgATP 5, EGTA 10, HEPES 10, pH was adjusted to 7.2 by CsOH).

Measurement of potassium currents

The inward rectifier (I_{K1}), transient outward (I_{to}), rapid (I_{Kr}) and slow (I_{Ks}) delayed rectifier and acetylcholine activated (I_{KACh}) potassium currents were recorded in HEPES-buffered Tyrode's solution. The composition of the pipette solution (in mM) was the following: KOH 110, KCl 40, K_2ATP 5, $MgCl_2$ 5, EGTA 5, HEPES 10 (pH was adjusted to 7.2 by aspartic acid). 1 µM nisoldipine was added to the bath solution to block I_{CaL}. When I_{Kr} was recorded I_{Ks} was inhibited by using the selective I_{Ks} blocker HMR-1556 (0.5 µM). During I_{Ks} measurements, I_{Kr} was blocked by 0.5 µM dofetilide and the bath solution contained 0.1 µM forskolin.

Since the run-down of I_{CaL} and I_{Ks} currents is commonly seen during the measurements, the current level was monitored during the initial equilibration period and also at the end of the measurements when a washout period of at least 10 min was applied in order to draw a distinction between drug effect and rundown of the current. The cells, in which excessive rundown was observed, were omitted from the analyses.

Measurement of late sodium current

The sodium current is activated by 2 s long depolarizing voltage pulses to -20 mV from the holding potential of -120 mV with pulsing cycle length of 5 s. After 5 - 7 min incubation with the drug the external solution was replaced by that containing 20 µM TTX. TTX at this concentration completely blocks the late sodium current (I_{NaL}). The external solution was HEPES-buffered Tyrode's solution supplemented with 1 µM nisoldipine, 0.5 µM HMR-1556 and 0.1 µM dofetilide in order to block I_{CaL}, I_{Ks} and I_{Kr} currents. The composition of the pipette solution (in mM) was: KOH 110, KCl 40, K_2ATP 5, $MgCl_2$ 5, EGTA 5, HEPES 10 (pH was adjusted to 7.2 by aspartic acid).

ECG measurements

ECG signals obtained from precordial leads were digitized and off-line analysed by using National Instruments data acquisition hardware (National Instruments, Austin, Texas, USA) and SPEL Advanced Haemosys software (version 3.2; Experimetria, Budapest, Hungary; MDE Heidelberg GmbH, Heidelberg, Germany). 30 consecutive beats (the minimum number of beats required for the calculation of beat-to-beat short-term variability of the RR and QT intervals; see below) were used to measure the mean PQ, QRS, RR, and QT intervals, respectively. The frequency-corrected QT interval (QTc) was calculated using the formula recommended specifically for Beagle dogs (Tattersall et al., 2006): QTc=QT-[0.087*(R–R-1000)].

Measurement of tissue and plasma AMIO and DEA levels by the HPLC method

Immediately following the sacrifice of the animals or completing the papillary muscle action potential measurements, and after 4 hours of myocyte isolation, samples were frozen in liquid nitrogen for subsequent high-performance liquid chromatography (HPLC) investigations. Cardiac (right and left atrial, right and left ventricular and left ventricular isolated myocyte suspensions), lung, kidney, liver tissue and plasma AMIO and DEA levels were determined from the samples by HPLC (Bolderman et al., 2009).

The Shimadzu HPLC system consisted of the following units: LC-20AD pump, DGU-20A3 degasser, SIL-20A HT auto sampler, CTO-20A column oven, SPD-M20A diode array detector. All data was collected and analyzed by Shimadzu LCsolution software. Chromatographic separation was performed at 35 °C on a Kromasil C8 column (5µm, 150 mm x 4.6 mm) protected by a C8 guard column using acetonitrile – 2-propanol – water – ammonia (80 : 10 : 10 :0.25, v/v) as mobile phase with UV detection at 245 nm. All measurements were done at a constant 1.00 ml/min flow rate.

Preparation of samples

For tissue sample preparation, 2.5 ml 0.01 M KH_2PO_4 (pH = 4.3) – methanol (75:25, v/v) solution was added to 1 gram of tissue. Tissue samples were homogenized with Janke & Kunkel Ultra-Turrax T25 homogenizer. 400 □l plasma or homogenized tissue sample was mixed with 20 □l tamoxifen (50 µg ml^{-1}) internal standard solution. The protein content of the sample was precipitated by 1.5 ml acetonitrile and the mixture was stirred for 1.5 minutes followed by a 10-minute centrifugation at 12 000 rpm at 4 ºC. The supernatant was evaporated to dryness under nitrogen atmosphere and the residue was dissolved in 100 □l eluent. 20 □l of this solution was injected into the HPLC system for each measurement.

Preparation of standard calibration solutions

Dog plasma calibration standards of AMIO and DEA (1 – 10 µg ml^{-1}) were prepared by spiking the working standard solutions (10 – 100 µg ml^{-1} in methanol) into a pool of drug-free dog plasma. Working standard solutions of AMIO and DEA were added to the drug-free tissue homogenate to prepare tissue calibration standards (5 – 500 µg g^{-1}). Calibration standards consisted of 400 µl of pooled drug-free plasma or tissue homogenate, 10 µl of AMIO or DEA working standard solution and 20 µl of tamoxifen (internal standard, 50 µg ml^{-1} in methanol). The rest of the sample preparation was the same as described above. Quality control samples (1, 5, 10 µg ml^{-1} and 5, 250, 500 µg g^{-1} for plasma and tissue samples, respectively) were prepared similarly.

qRT-PCR method

Left ventricular tissue samples were flash-frozen in liquid nitrogen and were stored at -80 ºC. To purify total RNA, ~100 mg of each tissue sample was homogenized in TRI reagent (Zymo Research, Irvine, California, USA) and was subjected to phenol-chlorophorm extraction. RNA was isolated from the aqueous phase using the Direct-Zol RNA MiniPrep (Zymo Research, Irvine, California, USA) following the manufacturer's instructions. RNA concentration was determined by UV-photometry. 2 µg of each RNA sample was reverse transcribed (RT) by using the High Capacity cDNA Reverse Transcription Kit (Zymo Research, Irvine, California, USA) with random oligomer primers following manufacturer`s instructions, 'noRT' control reactions were included to test for the presence of residual genomic DNA contamination. RNA samples with less than 10 threshold-cycle difference between cDNA and noRT control were excluded from the study.

SYBR-Green-based real-time PCR assays using the Maxima SYBR Green/ROX qPCR Master Mix (Waltham, Massachusetts, USA) were carried out on the AbiPrism7000

(Applied Biosystems, Foster City, California, USA) real-time PCR platform. PCR efficiencies were determined by 5-point relative standard curves using cDNA dilution series as template. Gene expression levels were normalized to the geometric average of the expression level of 5 housekeeping genes (SRP14, RPS5, ACTB, B2M, HPRT) for each sample.

Pharmacokinetics measurements

The major pharmacokinetic properties of DEA were determined and compared to those of AMIO after single dose of 25 mg kg^{-1} given intravenously and orally. For intravenous dosing, drugs were formulated in sulfobutylether-β-cyclodextrin and drug administration was performed in the form of short, 5-minute infusions. Oral doses were delivered by capsules after 24 h fasting. Blood samples were collected up to 48 hours post-dose and both DEA and AMIO levels were determined by the HPLC technique. Pharmacokinetic analysis was performed using Phoenix WinNonlin software version 6.3.

The individual plasma concentrations versus time curves were evaluated using non-compartmental method. Constant rate sort infusion and first order absorption methods were used for evaluation of the intravenous and oral curves, respectively.

The following parameters were calculated and partly presented: measured peak concentration (C_{max}), time of peak concentration (T_{max}), apparent terminal elimination half-life determined by software defined terminal phase fit ($t_{½}$), lagtime (T_{lag}), area under the curve from time zero to the last measurable concentration (AUC_{last}) and total AUC extrapolated to infinity (AUC_{inf}) calculated by linear trapezoidal integration and linear extrapolation, total clearance (Cl calculated as dose/AUC_{inf}), estimated volume of distribution at steady state (V_{ss} calculated as Cl*MRT_{inf}, where MRT_{inf} is the mean residence time), absolute oral bioavailability (F calculated as AUC_{inf_oral} / $AUC_{inf\_intravenous}$ expressed as

percentage) and metabolite/parent (DEA/AMIO) ratio of AUC_{inf} values expressed as percentage ($R_{D/A}$).

Exploratory, non-GLP chronic toxicological investigations

The oral dose of 25 mg kg^{-1} day^{-1} of DEA or AMIO was applied for 91 days to assess chronic toxicity in Beagle dogs. Two animals of both sexes were used in each group (n=4/group). Both DEA and AMIO were applied once a day, 7 days/week in gelatin capsules. The control animals (n=4/group) were treated in the same manner with placebo gelatin capsules. At the end of the study (91^{st} day), haematological and clinical chemistry investigations, a body weight measurement, ECG recording, urinary test, and following euthanization by sodium pentobarbital (30 mg kg^{-1}, i.v.; preceded by sedation using xylazine, 1 mg kg^{-1}, i.v.), autopsy and histopathological examinations were performed. In order to visualize connective tissue and for evaluation of pulmonary fibrosis, Crossmon's trichrome staining (Crossmon, 1937) was applied and a semi-quantitative scoring scale (according to the affected area and severity of alteration) was used by the evaluating pathologist, blinded to the treatment of individual dogs (0= no fibrosis, 1= moderate fibrosis, 2= severe fibrosis).

Data analysis

The data and statistical analysis comply with the recommendations of the British Journal of Pharmacology on experimental design and analysis in pharmacology (Curtis et al., 2018). Continuous variables are expressed as means ± SEM. Atrial fibrillation duration was expressed as log_{10} of AF duration in seconds for normal distribution of data. The "n" numbers shown on Figure panels and in the text and Tables refer to the number of dogs (i.e. individual data points represent the average value of measurements taken in preparations obtained from each dog and not the ventricular muscle preparations or cells).

Statistical analysis was performed by Microsoft Excel (RRID:SCR_016137, Microsoft Office Professional Plus 2016) and Power analysis was performed by Prism StatMate.

Group sizes - equal by design - were planned based on power calculations. The minimal number of animals per groups (DEA and AMIO groups) required for detecting a minimum 5% change (threshold of clinical relevance) in ECG parameters (such as 10 ms change in QT, for example) in response to the drug treatments compared to their baseline (drug-free, self-control) values (paired *t*-test, expected SD = 5% of the mean values of the different ECG parameters (SD = 10 ms in case of QT, for example)) at a 95% power level was n=6. On the other hand, to detect a minimum 5% difference in ECG parameters between AMIO and DEA treated groups (unpaired *t*-test, expected SD = 5% of the mean values of the different ECG parameters), at a 95% power level, a minimum of n=27 animals per groups were required. As after the *in vivo* ECG studies all of these AMIO and DEA treated animals were further used for *ex vivo* cellular and molecular biological experiments for which suitable control group was needed, another n=30 (age, weight and sex matched) dogs were assigned into the study as 'Control'. On the basis of such considerations, for the *in vivo* ECG and *ex vivo* cellular and molecular biological studies, we planned a sample size of minimum 27 animals for each group. Based on results obtained from previous experiments in which various anti-AF drugs were studied using the chronic atrial tachypacing-induced AF conscious dog models, we used the following expected values for the power analysis calculations for chi-square tests: expected proportion "success" (arrhythmia rate) in the control group = 0.70, significance level (alpha) = 0.05 (two-tailed), the required minimal proportion "success" (arrhythmia rate) after DEA administration that we needed to be able to detect was 0.35, which corresponds to a reduction of arrhythmia rate from 70% to 35%. Therefore, the minimal number of animals required for detecting at least 0.35 proportion

"success" (arrhythmia rate) after DEA administration at 80% power level was n=7, at 90% power level was n=9. Considering that these animal experiments require immense human and financial resources, conclusions gained at 80% power level appeared to be reasonable. For the acute carbachol induced canine AF model measurements, we chose the expected proportion "success" (arrhythmia rate) in the control group to be at least 0.85, the significance level (alpha) as 0.05 (two-tailed), and the required minimal proportion "success" (arrhythmia rate) after DEA administration (in the DEA group) that we needed to be able to detect was set to 0.35. Therefore, the minimal number of animals required for detecting at least 0.35 proportion "success" (arrhythmia rate) after DEA administration at 90% power level was n=6. Hence, n=6 control and n=6 (acute) DEA treated animals were used for these experiment.

The animals were assigned to the "groups" randomly. Age, weight and sex distribution of each group were designed to be equal. For the chronic atrial tachypacing-induced AF conscious dog experiments, only male animals were used as sex hormone levels (oestrogen and progesterone) in female animals during the long period of these chronic experiments could have had an influence on various cardiac ionic currents and thereby, on AF incidence.

The *in vivo* ECG and *ex vivo* cellular - intracellular AP and patch clamping - and molecular biological studies were performed in a blinded fashion: the investigators were not aware of the groups when performing experiments/analyses. The tissue AMIO and DEA level measurements were done by an investigator who was blinded to the treatment. Due to the nature of the experimental settings in case of the chronic atrial tachypacing-induced AF conscious dog model and the acute carbachol induced canine AF model measurements, where recordings were made before ('self-control') and following drug administration on the very same animals, blinding could not be undertaken.

The normal distribution of all data was checked prior to statistical analysis. To analyze normally distributed data, the following parametric tests were used: paired *t*-test for before vs. after treatment comparisons, and unpaired *t*-test for comparisons between independent groups. Chi-square test was used to compare the incidence of arrhythmias between different groups. Differences were considered significant when $p<0.05$.

Data points of restitution curves were fitted by a mono-exponential function in order to calculate the kinetic time constant of the APD_{90} restitution process:

$$APD = APDss - A*\exp(-DI/\tau)$$

where APDss is the maximal action potential duration (APD_{90}), A is the amplitude of the exponential function, DI is the diastolic interval and τ is the time constant. The curve fitting was performed by Origin software (RRID:SCR_014212, v2021, OriginLab).

Nomenclature of Targets and Ligands

Key protein targets and ligands in this article are hyperlinked to corresponding entries in http://www.guidetopharmacology.org, and are permanently archived in the Concise Guide to PHARMACOLOGY 2021/22 (Alexander et al., 2021).

RESULTS

In vivo electrophysiological and atrial antiarrhythmic effects of DEA

The effects of the acute i.v. (10 mg kg^{-1}) and the 4-week chronic oral DEA treatment (25 mg kg^{-1} day^{-1}) were studied in two dog models of AF: (i) in the intravenous carbachol infusion and rapid electrical burst induced acute AF model, and (ii) in the chronic atrial

tachypacing-induced atrial fibrillation model, respectively. Acute iv. application of 10 mg kg^{-1} DEA converted carbachol and burst induced sustained AF into sinus rhythm in 6 out of 6 experiments. Chronic DEA treatment significantly reduced the incidence of atrial tachypacing-induced AF to 35.8±11.6% (n=7, $p<0.05$) compared to those observed in control (70.7±10.1%), and decreased the average AF episode duration to 1.2±0.23 (expressed as $\log_{10}$ of AF duration in seconds, n=7, $p<0.05$) compared to those observed in control (2.3±0.18) i.e. before DEA treatment was initiated. Similarly, the total AF duration (expressed as $\log_{10}$ of AF duration in seconds) was also significantly reduced by chronic DEA treatment (1.7±0.39 *vs.* 3.2±0.14 in control, n=7, $p<0.05$). The AERP before the commencement of chronic atrial tachypacing in Beagle dogs was 119 ± 3.8 ms and 132 ± 4.2 ms (measured at 150 and 300 ms BCL, respectively; n=7). Importantly, chronic atrial tachypacing resulted in a marked decrease in AERP measured at both cycle lengths, however, the exact AERP could not be determined at this time point, since the AERP decreased to below 80 ms in all animals (the S1-S2 interval of 80 ms still evoked a P wave). This was due to a technical limitation of the pacemaker, since the lower limit for the S1-S2 intervals in the pacemakers was 80 ms. Therefore, statistical analysis of this parameter could not be performed. The AERP measurements yielded 88 ± 4.1 ms and 95 ± 5.0 ms following 25 mg kg^{-1} DEA treatment (measured at 150 and 300 ms BCL, respectively; n=7). Chronic (25 mg kg^{-1} day^{-1} once a day) DEA treatment resulted in moderate ECG parameter changes with relatively low corresponding plasma and tissue DEA levels as indicated in **Table 1**. To further study the plasma levels, tissue concentrations and cardiac electrophysiological effects of DEA, chronic oral DEA (25 mg kg^{-1} twice a day), and for comparison, AMIO (same dose) treatments were applied for 4 weeks. This higher dose was selected in order to have similar DEA and AMIO induced electrophysiological effects and plasma/tissue DEA and AMIO levels, which would better correspond to the steady-state tissue and plasma DEA and AMIO levels and ECG

changes reported earlier following longer, several months or years of AMIO treatment (Adams et al., 1985). At 2 x 25 mg kg^{-1} day^{-1} dose, both DEA and AMIO treatments significantly increased PQ, QRS, QT, QTc, and RR intervals and resulted in relatively high plasma and tissue drug concentrations **(Table 1)**. This higher dose, however, was still less than those reported in patients (Adams et al., 1985) after several months of drug application.

Effect of chronic oral DEA treatment on the action potentials

The effect of a 4-weeks oral DEA (25 mg kg^{-1} twice a day) treatment was studied on cardiac action potentials in atrial, ventricular muscle and Purkinje fibers by the conventional microelectrode technique. As **Table 2** shows, chronic DEA treatment markedly and to a similar extent increased the duration of repolarization measured as APD_{90} both in atrial and ventricular muscle preparations, without significantly changing APD_{90} in Purkinje fibers. Also, RP, APA and V_{max} were decreased by DEA application **(Table 2)**.

In ventricular papillary muscle, the effect on APD was dependent on the stimulation frequency i.e. the slower the applied stimulation frequencies were the more APD lengthening was observed **(FIG 1A)**.

The restitution of APD following chronic oral administration of DEA was measured in ventricular muscle by the double pulse protocol (S_1-S_2) with gradually increasing coupling diastolic intervals (DI) from the basic cycle length (S_1-S_2) of 1000 ms after every 20^{th} basic beat. As **FIG 1B** shows, DEA treatment significantly slowed the kinetics of restitution and also decreased the slope of the restitution curves.

Chronic DEA treatment, as **FIG 1C** shows, also decreased V_{max} in a frequency-dependent ("use-dependent") manner at cycle lengths shorter than 1000 ms.

The onset kinetics of this use-dependent V_{max} block after DEA treatment was relatively fast (**FIG 1D**), characterized by beat constants of 7.2±1.0 at the stimulation cycle

length of 400 ms. After the fast recovery of V_{max} of the drug free sodium channel having fast time constants of 24.8±2.0 ms in control and 36.4±11.0 ms in chronically DEA treated animals, respectively, in the papillary muscle obtained from chronically treated dogs a second slow recovery of V_{max} was observed with slow time constant of 687±155 ms, which was not noted in the control dogs (**FIG 1E**).

To assess the possible loss (washout) of DEA during the time course of the experiment, we determined the DEA concentrations in the papillary muscle preparations used for the action potential measurements after the end of the experiments. The DEA concentrations in these preparations (36.4±6.1 μg tissue g^{-1}, n=14) were not significantly different from those in right ventricular muscle samples (35.3±5.5 μg/tissue g, n=14), dissected from the same animals and frozen immediately after animals had been sacrificed. These data suggest that due to the high degree of lipophilicity of DEA, there was minimal diffusion of drug from the preparations during the time course of the study.

Effect of DEA on the dispersion of repolarization in the ventricle

The results showing that DEA prolongs APD in ventricular muscle but does not change APD in Purkinje fibers are strikingly different from the effects of Class III antiarrhythmic drugs. On **FIG 2**, the dispersion of repolarization between ventricular muscle and Purkinje fibers was compared after chronic DEA and acute sotalol (3 and 10 μM) – a widely used Class III antiarrhythmic drug - applications. As **FIG 2** shows, in spite of both DEA and sotalol markedly and significantly increasing APD in the papillary muscle, the dispersion of repolarization – defined here as differences in APD between Purkinje and ventricular muscle fibers – were considerably greater following sotalol application than following chronic DEA treatment, suggesting less potential proarrhythmic potential of DEA compared to that of sotalol.

Effect of acute DEA administration on dog action potentials

In some experiments, the effects of acute 10 µM DEA application in the tissue bath for 60-120 minutes on cardiac action potentials were also studied. This perfusion time was needed to achieve quasi steady-state drug effect. In dog right ventricular papillary muscle, as **FIG 3A** and **B** show, 10 µM acute DEA application exerted similar but less pronounced cycle length dependent changes on APD and V_{max} than those observed in right ventricular papillary muscles obtained from dogs chronically treated with DEA (**FIG 1**). No statistically significant changes were obtained in these parameters with 10 µM DEA in atrial muscle and Purkinje fibers. Also, in Purkinje fibers pretreated with 0.3 µM ouabain delayed afterdepolarizations (DAD) were evoked, and in 6 out of 6 experiments the DADs disappeared following acute application of 10 µM DEA (**FIG 3C**). These results are very similar to those reported by our laboratory earlier with similar acute administration of 10 µM AMIO (Varró et al., 2001).

To assess the drug accumulation in the tissue during acute drug superfusion, DEA concentration was measured in 20 right ventricular papillary muscle preparations exposed to 10 µM DEA in the tissue bath. In these preparations, after 98.3±13.9 minutes, 6.1±3.2 µg g^{-1} DEA concentration was measured. These results indicated that DEA concentrations were considerably lower in acute tissue experiments than those measured from chronically treated right ventricular tissue (35.6±3.8 µg g^{-1} DEA, n=26). The effect of 10 µM DEA developed slowly and as after the chronic treatment it was not reversible after several hours of washout.

Effect of DEA on transmembrane inward ionic currents

Inward late sodium current

The fast sodium current (I_{Naf}) is too large and fast and as such it cannot be measured directly in cardiac myocytes at 37 °C. Therefore, it was estimated by determining V_{max} of the action potential upstroke as shown previously in Figure 1C, D, E with the limitation of the fact that V_{max} is not linear index of I_{Naf} (Sheets et al., 1988).

The effect of chronic DEA treatment on the late sodium current (I_{NaL}) was measured by the patch-clamp technique. The slowly inactivating I_{NaL} was determined in ventricular myocytes at 2 s long test pulses of -20 mV after switching from the holding potential of -120 mV with pulsing cycle length of 5 s. Late I_{Na} was determined as the TTX (20 μM) sensitive difference current. As **FIG 4A** shows, the amplitude of I_{NaL} was somewhat but not significantly smaller measured in myocytes isolated from chronic DEA treated dogs compared to those obtained from non-treated control dogs without significantly changing the time course of its inactivation (83.6±5.6 ms, n=7 versus 88.4±4.7 ms, n=8). Acute, 3-5-minute application of 10 μM DEA produced an even stronger and statistically significant effect (**FIG 5A**).

Inward L-type calcium current

The effects of chronic DEA treatment on the inward L-type calcium current (I_{CaL}) are demonstrated on **FIG 4B**. At the pulse cycle length of 5 s, no difference was found in the amplitude of the I_{CaL} between untreated control myocytes and those obtained from dogs receiving chronic DEA treatment.

However, when pulse cycle length was shortened to 0.5 s, I_{CaL} was somewhat but not significantly smaller in ventricular myocytes obtained from chronic DEA treated animals compared to that measured in myocytes from untreated control dogs. To establish the rate-

dependent I_{CaL} block by DEA, trains of 40, 300-ms-long pulses to 0 mV were applied after a minute of stimulation-free period with a 500 ms pulse cycle length. In these measurements, significant rate-dependent I_{CaL} block was found in myocytes isolated from chronic DEA treated animals without significantly altering the inactivation kinetics of the current (at 0 mV 24.4±2.4 ms, n=5 versus 23.2±0.8 ms, n=5) and with significantly slower recovery kinetics from inactivation (99.2±5.8 ms, n=16 versus 166.6±11.2 ms, n=9). Similar but an even more pronounced effect was seen in acute experiments when 10 µM DEA was applied directly in the tissue bath for 3-5 minutes (**FIG 5B**).

The effect of DEA on outward potassium currents

In ventricular myocytes the chronic administration of DEA significantly decreased the inward rectifying (I_{K1}) and transient outward potassium currents (I_{to}) without significantly changing the inactivation kinetics of I_{to} (rapid component: 5.3±0.2 ms, n=16 versus 4.9±0.2 ms, n=9; slow component: 15.5±0.8 ms, n=16 versus 16.6±1.2 ms, n=9 at 50 mV) (**FIG 6A**). In acute experiments, however, 10 µM DEA did not influence I_{K1} and I_{to} currents. I_{K1} current was defined as the steady-state current at the end of a 300 ms test pulse with pulsing cycle length of 3 s in the voltage range of -100 to 0 mV. I_{to} was measured as the difference between peak current at the beginning of the 300 ms long depolarizing step and the steady-state current at the end of the pulse. The holding potential was -90 mV, while the pulsing cycle length was 3 s.

The acetylcholine-activated potassium current (I_{KACh}) was studied in atrial myocytes isolated from dogs chronically treated with DEA and isolated from untreated animals after acute DEA application (**FIG 6B**). In these experiments, 1000-ms-long ramp pulses were applied from -100 mV to 40 mV with a pulse cycle length of 2 s. The holding potential was -90 mV. The current was activated by 2 µM carbachol. The amplitude of I_{KACh} was measured

at -10 mV for outward current, as a tertiapin-sensitive difference current. As **FIG 6B** shows, I_{KACh} was significantly smaller in chronic DEA treated dogs than in controls. Acute DEA administration (**FIG 5C**) also depressed I_{KACh} with nearly to the same extent. The corresponding IC_{50} values after acute DEA administration were 1.1 ± 0.1 μM at -10 mV and 1.5 ± 0.1 μM at -100 mV, respectively.

The effects of DEA on rapid (I_{Kr}) and slow (I_{Ks}) delayed rectifier potassium currents were also studied in ventricular myocytes after chronic application. Chronic DEA treatment significantly decreased I_{Kr} and I_{Ks} currents in myocytes isolated from dogs after chronic oral treatment **(FIG 6C)**. The kinetic properties of these currents were not measured during chronic experiments except the deactivation kinetics of I_{Ks}, which was not changed by chronic administration of DEA (119.1±10.4 ms, n=9 versus 124.2±13.9 ms, n=7). During acute DEA (2 μM, 3.2 μM and 10 μM) application in myocytes obtained from non-treated dog hearts (**FIG 5D**) both I_{Kr} and I_{Ks} were also depressed in a concentration dependent manner (**FIG S1, S2** in Supporting Information). It has to be noted that the effect of DEA at concentration higher than 2 μM seemed pronounced after acute administration than in myocytes obtained from chronically treated dogs (IC_{50} for acute I_{Kr} inhibition = 4.1±0.5 μM; IC_{50} for I_{Ks} acute inhibition = 6.0±0.6 μM). The activation and deactivation kinetics of I_{Kr} and the activation kinetics of I_{Ks} – what was not measured during chronic experiments – were also calculated but they were not altered by acute application of 2 μM DEA (I_{Kr} activation: 32.6±5.0 ms, versus 31.6±8.8 ms, n=4; I_{Ks} activation: 493.0±57.5 ms, versus 457.0±109.9 ms, n=4 and I_{Kr} deactivation rapid component: 352.0±39.5 ms, versus 318.7±59.1 ms, n=3; I_{Kr} deactivation slow component: 4785±327 ms, versus 4721±156 ms, n=3). This DEA concentration (2 μM) measured after 20 min incubation of the myocytes with 2 μM DEA in separate experiments yielded 70.9±9.3 $\mu g\ g^{-1}$ (n=8) DEA concentration in the ventricular myocytes.

DEA accumulation in isolated single myocytes following chronic and acute treatments

In myocytes obtained from animals with chronic DEA treatment, the concentration of DEA after incubation in drug-free Tyrode solution was 30.8 ±5.1 μg g^{-1}, n=6. Acute DEA application in cardiomyocytes isolated from non-treated control dogs was also studied by incubating with 1.6 μM 2 μM, 3.2 μM and 10 μM DEA for 20 minutes. In these myocyte preparations, DEA concentrations were 19.6±5.6 μg g^{-1} n=12, 70.9±9.3 μg g^{-1} n=8, 101.4±12.8 μg g^{-1} n=12 and 119.9±53.8 μg g^{-1} n=11. These results suggest that due to the unrestricted diffusion - unlike in tissue experiments - high degree of DEA accumulation was observed in control myocytes after 20 min acute 1.6 μM 2 μM, 3.2 μM and 10 μM DEA application than those measured in the papillary muscle tissue preparations. These cellular DEA concentrations seem in a reasonable agreement with the results obtained from acute and chronic DEA experiments and from tissue action potential and cellular transmembrane ion current measurements.

Amiodarone and desethylamiodarone levels in the plasma and their accumulation in various tissues

FIG 7A shows the AMIO and DEA plasma levels and their accumulation in different tissue types, including the heart, in dogs following 4-week 50 mg kg^{-1} AMIO or DEA treatments. In the plasma, in AMIO treated dogs the AMIO concentration was higher (6.0 ± 0.6 μg ml^{-1}, n=27) than that of its metabolite, DEA (1.2 ± 0.2 μg ml^{-1}, n=27). This latter was very similar than that of in DEA treated animals (0.96 ± 0.1 μg ml^{-1}, n=19). However, the corresponding values for AMIO and DEA levels in various tissue types seemed comparable following chronic AMIO and DEA treatments. It is important to consider that the total drug (DEA + AMIO) accumulation was significantly lower in DEA treated animals than in those

treated with similar doses of AMIO, while DEA treatment exerted very similar cardiac electrophysiological effects compared to AMIO treatment.

The effect of chronic DEA treatment on the expression of different ion channels

The effects of chronic DEA treatment on the expression of different ion channels were studied by the qPCR technique in left ventricular tissue samples obtained and immediately frozen from control and chronic DEA treated dogs. **FIG 7B** shows that chronic DEA treatment did not significantly alter the mRNA levels of SCNA5/Nav1.5, KCNA4/Kv1.4, CACNA1C/Cav1.2, KCNJ4/Kir2.3 KCND3/Kv4.3, KCNQ1/KvLQT1, KCNJ2/Kir2.1, KCNE2/MirP1 and only moderately but significantly enhanced the mRNA levels of KCNH2/hERG, KCNIP2/KChIP2 and KCNE1/minK subunits.

Major pharmacokinetic properties of DEA and AMIO

The major pharmacokinetic properties of DEA were determined and compared to those of AMIO after a single dose of 25 mg kg^{-1} given intravenously and orally. The results are summarized in **Table 3**.

Following intravenous administration AMIO showed substantially greater maximum plasma concentration (C_{max}) and area under the curve (AUC) compared to those of DEA. This fact indicated faster and more intense penetration of DEA into tissue and organs resulting in larger volume of distribution than that of AMIO. Following oral administration DEA showed considerably higher (about double) bioavailability than that of AMIO, but the oral plasma exposure of DEA also remained lower due to its better distribution and more intense elimination properties than that of AMIO. The total clearance of DEA was also markedly (4-fold) higher compared to that of AMIO.

Exploratory, non-GLP chronic toxicological investigations with DEA and AMIO

The oral dose of 25 mg kg^{-1} day^{-1} of DEA (n=4) or AMIO (n=4) was applied for 91 days to assess chronic toxicity in Beagle dogs. No death has occurred and the body weights of the animals did not change in any of the 3 groups during the investigational period. No significant macroscopic alterations and focal lesions were found in the heart, liver, spleen, kidneys, pancreas, stomach, intestines, brain, thyroid gland, eyeball, lymph node, skeletal muscle and gonads. In the lung, histopathological studies with trichrome stain showed alterations in the DEA and AMIO treated groups, 4 moderate perivascular fibrosis without significant interstitial fibrosis in 4 DEA treated dogs while 4 serious interstitial fibrosis was seen in all AMIO (n=4) treated dogs (**FIG 7C** and**_Supplementary FIG S3**). No histopathological changes were observed in the control dogs. The clinical chemistry investigations did not show significant alterations between the control, DEA and AMIO groups. Importantly, haematological studies revealed marked leukocytopenia in the AMIO treated dogs (5.4±2.5 G l^{-1} versus 13.8±1.33 G l^{-1}, $p<0.05$) while no significant changes in leukocyte numbers were found in the control (10.7±1.80 G l^{-1} versus 10.1±1.84 G l^{-1}) and DEA treated (11.16±1.76 G l^{-1} versus 11.36±2.42 G l^{-1}) animals. The leukocytopenia was due to marked neutropenia in the AMIO treated dogs (1.14±1.09 G l^{-1} versus 6.78±1.52 G l^{-1}) as it has been reported earlier in a clinical report (Groneberg and Barkhuizen, 2001).

DISCUSSION

In this study, we investigated the acute and chronic electrophysiological and antiarrhythmic effects of DEA, the main metabolite of AMIO, in dogs.

The main novel findings of the present study are the following:

1. We provided the first experimental evidence that DEA treatment exerts antiarrhythmic effects in a large animal model of atrial fibrillation.

2. We report for the first time using a comprehensive approach by measuring action potentials, various transmembrane ionic currents and expression of ion channels that chronic DEA treatment exerts similar effects on potassium and sodium currents as it was previously reported for its parent compound AMIO (Varró et al., 2001; Sun et al., 1999; Sosunov et al., 1996; Bosch et al., 1999).

3. DEA treatment in equal doses of AMIO causes similar ECG effects, however, produces lower drug exposition. Also, DEA treatment is associated with more favorable pharmacokinetics than its parent compound AMIO. In addition, since DEA seem to cause less hematological and pulmonary side effects than its parent compound AMIO, we suggest to consider testing DEA in clinical trials for the management of cardiac arrhythmias including atrial fibrillation.

The applied doses and concentrations of DEA and AMIO in the present study were similar to those of reported in previous animal studies on rabbit and canine (Varró et al., 2001; Sun et al., 1999; Kato et al., 1988) but higher than the doses regularly applied in human therapy with AMIO (Mujović et al., 2020). It has to be emphasized, however, that in our present and in other previous animal studies (Varró et al., 2001; Sun et al., 1999; Kato et al., 1988), the duration of the treatment was much shorter (4 weeks) than the usual length of the treatment in patients (several months or years) and considerable pharmacological differences may exist between beagle dogs and human. Accordingly, in spite of the relatively high dose compared to the clinical studies, the tissue accumulation of AMIO and DEA were lower or similar in our experiments to those reported (Adams et al., 1985) by biopsy or autopsy in clinical studies.

There is ample evidence from animal experiments (Sosunov et al., 1996) and in patients (Mujović et al., 2020) showing that acute and chronic (Kudenchuk et al., 1999; Sosunov et al., 1996; Morvay et al., 2015) AMIO therapy is effective against atrial fibrillation and other types of arrhythmias as well. It has also been known for a long time that AMIO has an active metabolite, DEA (Kodama et al., 1999). Surprisingly, however, there are no published data regarding the effects of DEA in atrial fibrillation. Also, only few studies reported the antiarrhythmic effect of DEA in ventricular arrhythmias following acute application (Varró et al., 1987), and only one recent study (Morvay et al., 2015) reported the effectiveness of chronic DEA administration in coronary artery occlusion induced ventricular arrhythmias in conscious rats. The limited number of available cardiac electrophysiological measurements with DEA (Talajic et al., 1987; Kato et al., 1988; Yabek et al., 1986; Stark et al., 1991) showed strong similarity with its parent compound AMIO (Mason et al., 1984; Nishimura et al., 1989; Kodama et al., 1992; Varró et al., 1996; Ghovanloo et al., 2016). However, all of these data with DEA – with the exception of an early study on rabbit action potential (Kato et al., 1988) – were obtained following acute application.

In general, the results in the present study are in good agreement with the few earlier studies reported with acute DEA and AMIO administration (Kato et al., 1988; Sun et al., 1999; Sosunov et al., 1996; Yabek et al., 1986; Nishimura et al., 1989; Kodama et al., 1992). The present results suggest that the strong electrophysiological effects of chronic DEA treatment were due to its high tissue concentration and DEA did not diffuse from the preparations during the time course of the experiments. Importantly, strong antiarrhythmic and electrophysiological effects were achieved by DEA treatment alone which associated with reduced total drug exposition and less toxicity compared to AMIO treatment with a similar dose. These results were the base of a successful DEA patent application (Varró et al., 2013). In addition, DEA was reported to cause venodilation in humans (Grossmann et al.,

2000). This effect, particularly during intravenous administration, is expected to reduce atrial stretch, potentially contributing to the antiarrhythmic effect.

The differences in the pharmacokinetic properties between DEA and AMIO are interesting findings, since their physicochemical properties seem to be similar. The higher bioavailability and greater volume of distribution make DEA favorable to apply both orally and intravenously. Also, it was reported that DEA could decrease the transformation of AMIO into DEA (Seki et al., 2008), which can indirectly decrease the elimination of AMIO, possibly contributing to additional tissue drug accumulation.

The observed DEA and AMIO induced changes in ECG parameters, action potentials and transmembrane ion currents with the exception of I_{K1} and I_{to} could be well explained by the direct interactions of these drugs with ion channels as suggested in an earlier study (Bosch et al., 1999) where no particular evidence was found for a meaningful electrophysiological remodeling. In the contrary, thyroid receptor related remodeling was suggested by Kodama and Latham (Kodama et al., 1999; Latham et al., 1987) and changed mRNA expression was reported following long term AMIO administration in the mouse heart (Le Bouter et al., 2004). The observed discrepancies between the results of the mRNA and patch clamp experiments after chronic DEA treatment in the present study are unknown and may reflect changes in the corresponding channel protein translation or signaling process. Therefore, further studies in this direction would be necessary. The bradycardia, PQ interval lengthening, reduction of repolarization heterogeneity between ventricular muscle and Purkinje fibers induced by DEA and AMIO can be best explained by an effect on the L-type calcium and late sodium currents, however, the role of the beta adrenergic receptors cannot be ruled out. The widening of the QRS interval, use-dependent decrease of V_{max} observed in ventricle are consistent with the direct inhibition of the drug on the fast sodium current. The DEA induced slowing of recovery of V_{max} was relatively rapid like with Class I/B sodium

channel blocking drugs like mexiletine and lidocaine and previously reported by dronedarone and amiodarone (Varró et al., 2001; Kato et al., 1988; Mason et al., 1984). The significant prolongation of the QT interval on the ECG and prolongation of the APD in ventricular and atrial muscle can be attributed to the drug induced inhibition of I_{Kr}, I_{to} and I_{Ks}. The so far unrecognized effects of DEA on the kinetics of APD restitution can relate to their lengthening of repolarization as suggested by Shattock et al. (2017) but the contribution of the use-dependent effects by DEA on I_{Na} and I_{CaL} cannot be ruled out either (Árpádffy-Lovas et al., 2020). All these discussed effects and the observed I_{KACh} inhibition by DEA can play significant roles in the effectiveness of DEA in preventing and abolishing atrial fibrillation in our dog model of AF. In addition, DEA was reported to affect intracellular Ca^{2+} handling as well, possibly impacting cardiomyocyte electrophysiology and function (Himmel et al., 2000). In general, it seems that the electrophysiological effects of DEA in this study are similar to those reported earlier by a large number of previous studies with AMIO (Talajic et al., 1987; Nattel et al., 1988; Sun et al., 1999; Sosunov et al., 1996; Nishimura et al., 1989; Kodama et al., 1992) and by a few studies with acute DEA application (Kato et al., 1988; Yabek et al., 1986; Stark et al., 1991; Varró et al., 1996).

LIMITATIONS OF THE STUDY

The role of AMIO in the treatment of AF is declining because of the numerous and often serious side effects of AMIO. The point, therefore, how the advantageous toxicological observations in the present study with DEA would be manifested in patients still represents further uncertainty. In addition, differences can also be expected in the pharmacokinetics including drug accumulation between diseased humans and Beagle dogs. Therefore, it is possible that in spite of the improved pharmacokinetic and toxicological features of DEA over AMIO, the relatively low number of observations in animal experiments may not

generate enough interest to initiate large, controlled clinical studies with DEA, but further detailed animal experimental studies with DEA, including further characterization of its atrial cellular electrophysiological effects, and studies in limited number of patients should be performed to resolve this issue.

CONCLUSION

Based on our present results, it is concluded that similar antiarrhythmic and cardiac electrophysiological effects can be achieved with DEA administration as it was reported earlier with AMIO application. However, the total drug exposition, the hematological and potential organ toxicity observed in the present animal experiments were lower following DEA application than those after AMIO treatment. In addition, DEA has more favorable pharmacokinetic properties. These results can justify the initiation of clinical trials to establish the possible therapeutic advantages of DEA over AMIO in patients.

ACKNOWLEDGEMENTS

This work was supported by the National Research Development and Innovation Office (NKFIH K 119992, NKFIH PD-125402 and FK-129117 (to NN), NKFIH K 128851 (to IB) and GINOP-2.3.2.-15-2016-00048 and the TKP2021-EGA-32), the Ministry of Human Capacities Hungary (20391 3/2018/FEKUSTRAT and EFOP-3.6.2-16-2017-00006), the UNKP-20-5-SZTE-165, János Bolyai Research Scholarship of the Hungarian Academy of Sciences (to NN) and by the Albert Szent-Györgyi Medical School institutional grant (SZTE ÁOK-KKA 2021 to LV).

AUTHOR CONTRIBUTIONS

L.V., I.B. and A.V. conceived the experiments. Zs.K., T.H., Z.H., A. Sz-I., N.N., A.H., R.V., J.P., J.Sz., N.T. P.G., M.N., T.Á-L., B.P., T.M., I.K., Sz.D., V.D-H., B.Ö., L.T., L.To., L.Ti., Z.A. and I.F. conducted the measurements. Zs.K., T.H., Z.H., A. Sz-I., N.N., A.H., R.V., J.P., J.Sz., P.G., T.Á-L., B.P., T.M., I.K., Sz.D., V.D-H., B.Ö., L.V., M.P. and I.B. analyzed the results. Zs.K., L.V., M.P., L.Ti., N.J., I.B., and A.V. prepared the manuscript. All authors reviewed and agreed to the content of the manuscript.

CONFLICT OF INTEREST

The authors declare no conflicts of interest.

A.V., I. B., N. J., A.Sz-I., L.V. are inventors of the successful patent application of DEA (Varró et al., 2013).

DECLARATION OF TRANSPARENCY AND SCIENTIFIC RIGOUR

This Declaration acknowledges that this paper adheres to the principles for transparent reporting and scientific rigour of preclinical research as stated in the BJP guidelines for Design and Analysis, and Animal Experimentation, and as recommended by funding agencies, publishers and other organisations engaged with supporting research.

REFERENCES

Adams PC, Holt DW, Storey GC, Morley AR, Callaghan J, Campbell RW. (1985). Amiodarone and its desethyl metabolite: tissue distribution and morphologic changes during long-term therapy. *Circulation* 72(5):1064-75.

Alexander SP, Mathie A, Peters JA, Veale EL, Striessnig J, Kelly E, et al. (2021). THE CONCISE GUIDE TO PHARMACOLOGY 2021/22: Ion channels. British Journal of Pharmacology 178(S1): S157-S245.

Árpádffy-Lovas T, Baczkó I, Baláti B, Bitay M, Jost N, Lengyel Cs, et al. (2020). Electrical restitution and its modifications by antiarrhythmic drugs in undiseased human ventricular muscle. *Front Pharmacol* 11:479. doi: 10.3389/fphar.2020.00479.

Baczko I, Liknes D, Yang W, Hamming KC, Searle G, Jaeger K, et al. (2014). Characterization of a novel multifunctional resveratrol derivative for the treatment of atrial fibrillation. *Br J Pharmacol*. 171(1):92-106.

Bolderman RW, Hermans JJR, Maessen JG. (2009). Determination of the class III antiarrhythmic drugs dronedarone and amiodarone, and their principal metabolites in plasma and myocardium by high-performance liquid chromatography and UV-detection. J Chromatogr B. 877: 1727-31. doi:10.1016/j.jchromb.2009.04.029

Bosch RF, Li GR, Gaspo R, Nattel S. (1999). Electrophysiologic effects of chronic amiodarone therapy and hypothyroidism, alone and in combination, on guinea pig ventricular myocytes. *J Pharmacol Exp Ther* 289(1):156-65.

Crossmon G. (1937). A modification of Mallory's connective tissue stain with a discussion of the principles involved. Anat. Rec. 69:33–38.

Curtis MJ, Alexander S, Cirino G, Docherty JR, George CH, Giembycz MA, Hoyer D, Insel PA, Izzo AA, Ji Y, MacEwan DJ, Sobey CG, Stanford SC, Teixeira MM, Wonnacott S,

Ahluwalia A. (2018). Experimental design and analysis and their reporting II: updated and simplified guidance for authors and peer reviewers. *Br J Pharmacol*. 175(7):987-993.

Ghovanloo MR, Abdelsayed M, Ruben PC. (2016). Effects of Amiodarone and N-desethylamiodarone on Cardiac Voltage-Gated Sodium Channels. *Front Pharmacol* 7:39.

Groneberg DA, Barkhuizen A. Neutropenia during treatment with amiodarone. *Am J Med* 2001;110(8):671.

Grossmann M, Dobrev D, Himmel HM, Kirch W. (2000). Local venous response to N-desethylamiodarone in humans. *Clin Pharmacol Ther* 67(1):22-31. doi: 10.1067/mcp.2000.103822. PMID: 10668850

Himmel HM, Dobrev D, Grossmann M, Ravens U. (2000). N-desethylamiodarone modulates intracellular calcium concentration in endothelial cells. *Naunyn Schmiedebergs Arch Pharmacol* 362(6):489-96. doi: 10.1007/s002100000301.

Jost N, Nagy N, Corici C, Kohajda Z, Horváth A, Acsai K, Biliczki P, Levijoki J, Pollesello P, Koskelainen T, Otsomaa L, Tóth A, Papp JG, Varró A, Virág L. (2013). ORM-10103, a novel specific inhibitor of the Na+/Ca2+ exchanger, decreases early and delayed afterdepolarizations in the canine heart. *Br J Pharmacol*. 170(4):768-78. doi: 10.1111/bph.12228.

Kato R, Venkatesh N, Kamiya K, Yabek S, Kannan R, Singh BN. (1988). Electrophysiologic effects of desethylamiodarone, an active metabolite of amiodarone: comparison with amiodarone during chronic administration in rabbits. *Am Heart J* 115:351-359. doi: 10.1016/0002-8703(88)90481-4.

Kavousi M. (2020). Differences in Epidemiology and Risk Factors for Atrial Fibrillation Between Women and Men. *Front Cardiovasc Med* 7:3. doi: 10.3389/fcvm.2020.00003.

Kilkenny C, Browne W, Cuthill IC, Emerson M, Altman DG, NC3Rs Reporting Guidelines Working Group. (2010). Animal research: reporting in vivo experiments: the ARRIVE guidelines. *Br J Pharmacol*. 160(7):1577-9. doi: 10.1111/j.1476-5381.2010.00872.x.

Kodama I, Kamiya K, Toyama J. (1999). Amiodarone: ionic and cellular mechanisms of action of the most promising class III agent. *Am J Cardiol* 84:20R-28R.

Kodama I, Suzuki R, Kamiya K, Iwata H, Toyama J. (1992). Effects of long-term oral administration of amiodarone on the electromechanical performance of rabbit ventricular muscle. *Br J Pharmacol* 107(2):502-9.

Kudenchuk PJ, Cobb LA, Copass MK, Cummins RO, Doherty AM, Fahrenbruch CE, et al. (1999). Amiodarone for resuscitation after out-of-hosHimmpital cardiac arrest due to ventricular fibrillation. *N Engl J Med* 341(12): 871-8.

Latham KR, Sellitti DF, Goldstein RE. (1987). Interaction of amiodarone and desethylamiodarone with solubilized nuclear thyroid hormone receptors. *J Am Coll Cardiol* 9:872-876. doi: 10.1016/S0735-1097(87)80244-9.

Le Bouter S, El Harchi A, Marionneau C, Bellocq C, Chambellan A, van Veen T, Boixel C, Gavillet B, Abriel H, Le Quang K, Chevalier JC, Lande G, Léger JJ, Charpentier F, Escande D, Demolombe S. (2004). Long-term amiodarone administration remodels expression of ion channel transcripts in the mouse heart. *Circulation* 110(19):3028-35. doi: 10.1161/01.CIR.0000147187.78162.AC.

Mason JW, Hondeghem LM, Katzung BG. (1984). Block of inactivated sodium channels and of depolarization-induced automaticity in guinea pig papillary muscle by amiodarone. *Circ Res* 55(3):278-85.

McGrath JC, Lilley E. (2015). Implementing guidelines on reporting research using animals (ARRIVE etc.): new requirements for publication in BJP. *Br J Pharmacol*. 172(13):3189-93. doi: 10.1111/bph.12955.

Morvay N, Baczkó I, Sztojkov-Ivanov A, Falkay Gy, Papp JGy, Varró A, et al. (2015). Long-term pretreatment with desethylamiodarone (DEA) or amiodarone (AMIO) protects against coronary artery occlusion induced ventricular arrhythmias in conscious rats. *Can J Physiol Pharmacol* 93:773-7777. doi: 10.1139/cjpp-2014-0530

Mujović N, Dobrev D, Marinković M, Russo V, Potpara TS. (2020). The role of amiodarone in contemporary management of complex cardiac arrhythmias. *Pharmacol Res* 151:104521.

Nattel S, Davies M, Quantz M. (1988). The antiarrhythmic efficacy of amiodarone and desethylamiodarone, alone and in combination, in dogs with acute myocardial infarction. *Circulation* 77(1):200-8.

Nishimura M, Follmer CH, Singer DH. (1989). Amiodarone blocks calcium current in single guinea pig ventricular myocytes. *J Pharmacol Exp Ther* 251(2):650-9.

Seki S, Itagaki S, Kobayashi M, Hirano T, Iseki K. (2008). Amiodarone increases the accumulation of DEA in a human alveolar epithelium-derived cell line. *Biol Pharm Bull* 31(7):1449-52.

Shattock MJ, Park KC, Yang HY, Lee AWC, Niederer S, MacLeod KT, et al. (2017). Restitution slope is principally determined by steady-state action potential duration. *Cardiovasc Res* 113(7):817-828.

Sheets MF, Hanck DA, Fozzard HA. (1988). Nonlinear relation between Vmax and INa in canine cardiac Purkinje cells. *Circ Res* 63:386-398.

Shomanova Z, Ohnewein B, Schernthaner C, Höfer K, Pogoda CA, Frommeyer G, et al. (2020). Classic and Novel Biomarkers as Potential Predictors of Ventricular Arrhythmias and Sudden Cardiac Death. *J Clin Med* 9(2):578. pii: E578.

Sosunov EA, Anyukhovsky EP, Rosen MR. (1996). Chronic in vivo and in vitro effects of amiodarone on guinea pig hearts. *J Pharmacol Exp Ther* 278:906-912.

Stark G, Stark U, Windisch M, Vicenzi M, Eggenreich U, Nagl S, et al. (1991). Comparison of acute electrophysiological effects of amiodarone and its metabolite desethylamiodarone in Langendorff perfused guinea pig hearts. *Basic Res Cardiol* 86(2):136-47.

Sun W, Sarma JS, Singh BN. (1999). Electrophysiological effects of dronedarone (SR33589), a noniodinated benzofuran derivative, in the rabbit heart: comparison with amiodarone. *Circulation* 100:2276-2281.

Talajic M, DeRoode MR, Nattel S. (1987). Comparative electrophysiologic effects of intravenous amiodarone and desethylamiodarone in dogs: evidence for clinically relevant activity of the metabolite. *Circulation* 75(1):265-71.

Tattersall ML, Dymond M, Hammond T, Valentin JP. (2006). Correction of QT values to allow for increases in heart rate in conscious Beagle dogs in toxicology assessment. J Pharmacol Toxicol Methods. 53: 11–19.

Varró A, Bódi I, Rabloczky G. (1987). Antiarrhythmic effect of desethylamiodarone in conscious rats. *J Pharm Pharmacol* 39(6):483-4.

Varró A, Matyus P, Baczko I, Falkay Gy, Jost N, Lepran I, Sztojkov-Ivanov A, Virag L, Buzas N. (2013). Treatment and prevention of cardiac arrhythmias. EPO, Patent No: 2674158.

Varró A, Takács J, Németh M, Hála O, Virág L, Iost N, et al. (2001). Electrophysiological effects of dronedarone (SR 33589), a noniodinated amiodarone derivative in the canine heart: comparison with amiodarone. Br J Pharmacol. 133: 625-634.

Varró A, Virág L, Papp JG. (1996). Comparison of the chronic and acute effects of amiodarone on the calcium and potassium currents in rabbit isolated cardiac myocytes. *Br J Pharmacol*. 117(6):1181-6. doi: 10.1111/j.1476-5381.1996.tb16713.x

Yabek SM, Kato R, Singh BN. (1986). Effects of amiodarone and its metabolite, desethylamiodarone, on the electrophysiologic properties of isolated cardiac muscle. *J Cardiovasc Pharmacol* 8(1):197-207.

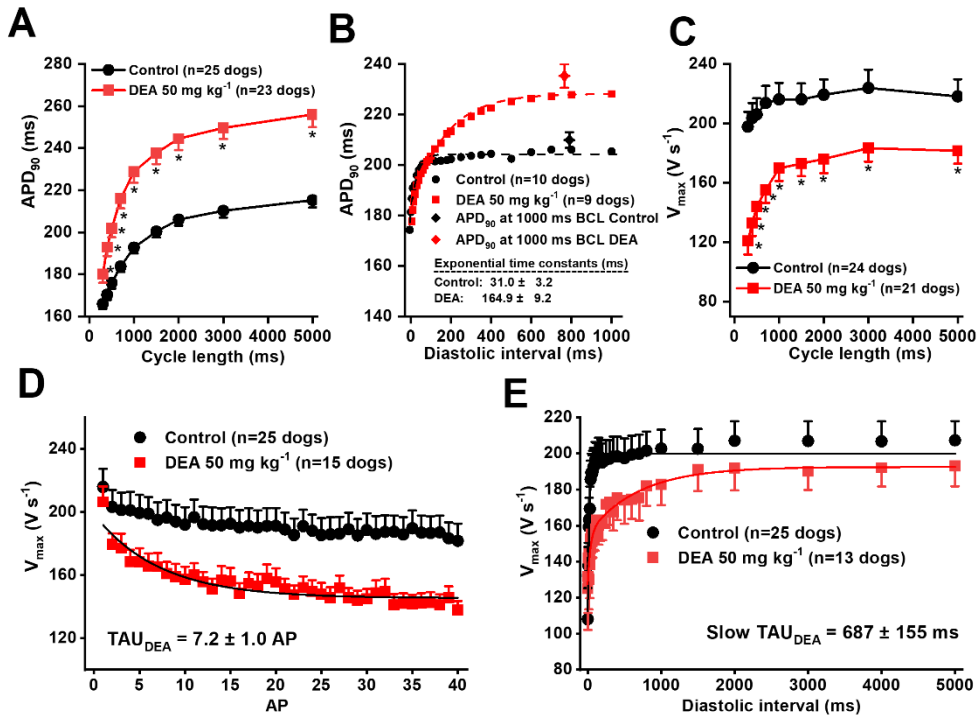

Figure 1. Effect of chronic oral DEA treatment on the frequency dependent APD and on V_{max} in dog ventricular muscle preparations. Panels **A** and **B** show the effects of chronic DEA application on APD_{90} at different steady state cycle lengths (n=25 dogs for control group and n=23 dogs for DEA group, average of 1 – 6 preparations for each dog) and on the restitution of APD_{90} (n=10 dogs for control group and n=9 dogs for DEA group, average of 1 – 5 preparations for each dog), respectively. Black and red diamonds in panel **B** indicate APD_{90} at 1000 ms basic cycle length in control (n=29 dogs, average of 1 – 5 preparations for each dog) and in DEA treated groups (n=24 dogs, average of 1 – 6 preparations for each dog), respectively. In panel **C** the steady state cycle length dependent effects of chronic DEA administration on V_{max} are shown in dog ventricular muscle preparations (n=24 dogs for control group and n=21 dogs for DEA group, average of 1 – 6 preparations for each dog). Panels **D** and **E** indicate the onset and offset kinetics of V_{max} block elicited by chronic DEA treatment, respectively (onset kinetics: n=25 dogs for control

group and n=15 dogs for DEA group, average of 1 – 5 preparations for each dog; offset kinetics: n=25 dogs for control group and n=13 dogs for DEA group, average of 1 – 4 preparations for each dog). In both measurements the basic stimulation cycle length was 400 ms. The "n" numbers refer to the number of dogs, data are expressed as means ± SEM.

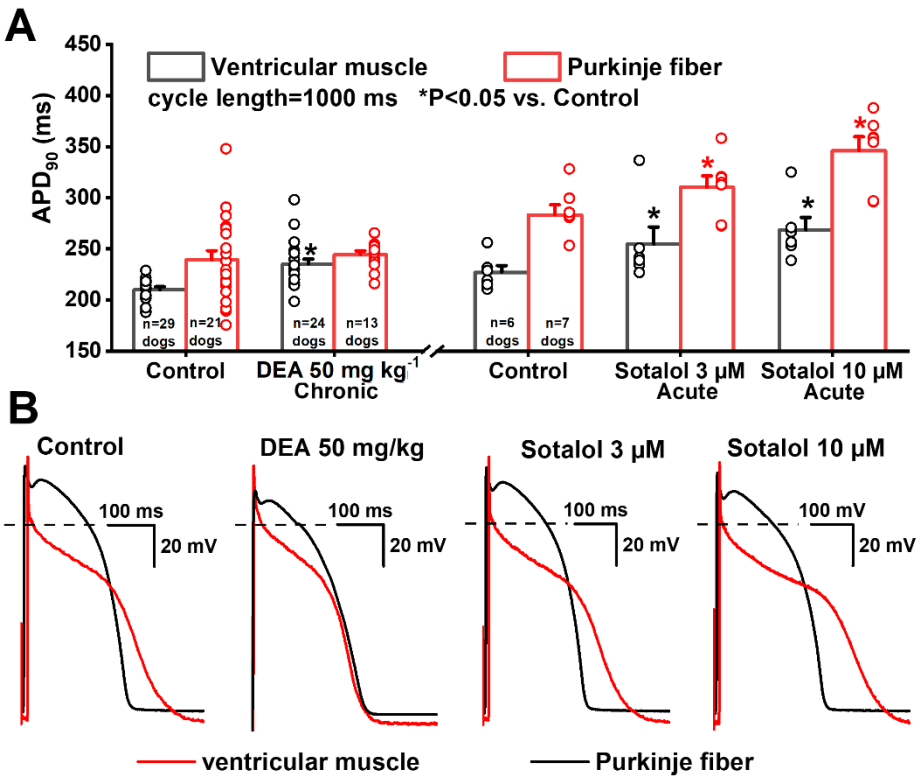

Figure 2. Effect of DEA on the dispersion repolarization in the ventricle and Purkinje fibers. In panel **A** dispersion of repolarization between ventricular muscle and Purkinje fiber is compared in untreated (control, n=29 dogs for ventricular muscle and n=21 dogs for Purkinje fiber, average of 1 – 5 preparations for each dog), chronic DEA treated dogs (n=24 dogs for ventricular muscle and n=13 dogs for Purkinje fiber, average of 1 – 6 preparations for each dog) and in preparations after application of 3 and 10 µM sotalol (n=6 dogs for ventricular muscle and n=7 dogs for Purkinje fiber, 1 preparation per dog). Open circles indicate individual data points for each dog. In panel **B** original action potential recordings from right ventricular muscle preparations and from Purkinje fibers are shown in untreated (1st panel from left), chronic DEA treated dogs (2nd panel) and in the presence of 3 and 10 µM sotalol (3rd and 4th panel from left). The "n" numbers refer to the number of dogs, data are expressed as means ± SEM.

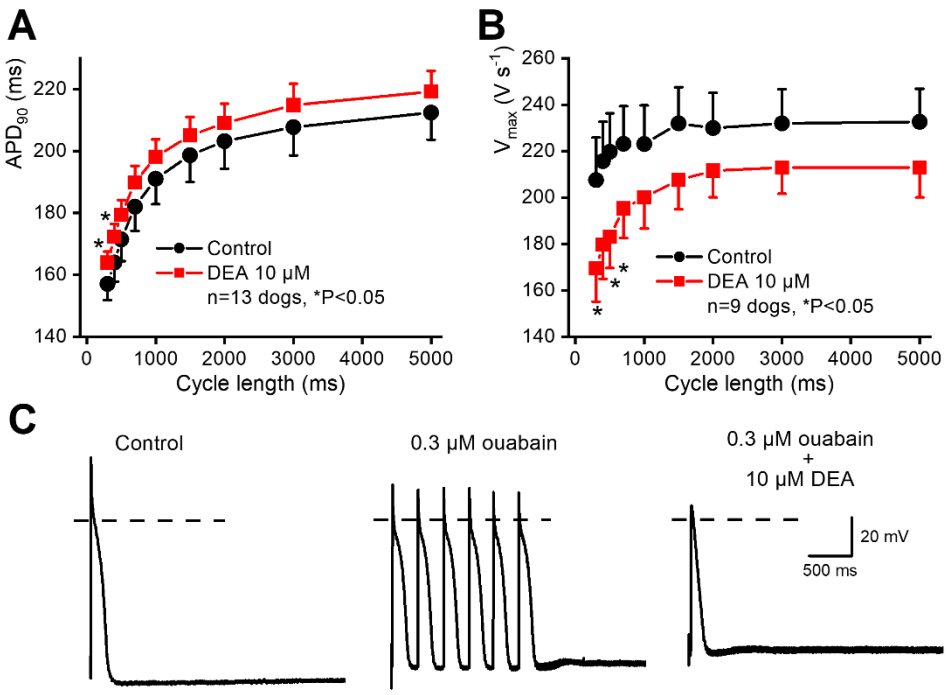

Figure 3. Effect of acute DEA administration on dog ventricular action potentials. Cycle length dependent effects of acute DEA administration on APD_{90} (n=13 dogs, average of 1 – 2 preparations for each dog) and V_{max} (n=9 dogs, average of 1 – 2 preparations for each dog) are shown in panel **A** and **B**, respectively, in dog ventricular muscle preparations. Panel **C** indicates the effect of acute DEA administration on ouabain induced delayed afterdepolarizations (DAD) in dog Purkinje fibers. The "n" numbers refer to the number of dogs, data are expressed as means ± SEM.

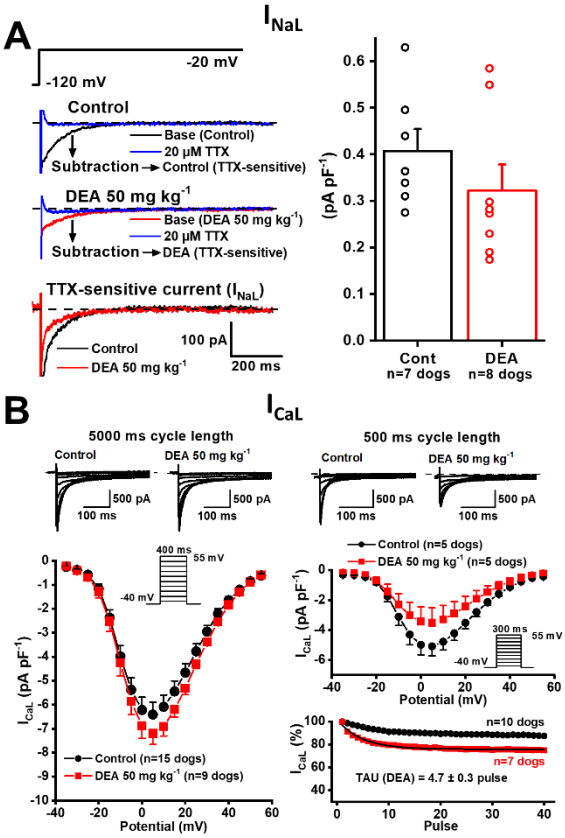

Figure 4. Effect of chronic DEA treatment on late sodium and L-type calcium currents. Effects of chronic DEA administration on I_{NaL} current in dog ventricular myocytes are indicated showing original current records (left) and bar diagrams (right) in panel **A** (n=7 dogs for control group and n=8 dogs for DEA group, average of 1 – 6 cells for each dog). Open circles indicate individual data points for each dog. Panels in **B** indicate original current records (top) and current-voltage relationship of I_{CaL} recorded with 5000 ms (n=15 dogs for control group and n=9 dogs for DEA group, average of 1 – 7 cells for each dog) and 500 ms pulsing cycle length (n=5 dogs for control group and n=5 dogs for DEA group, average of 1 – 6 cells for each dog) in myocytes isolated from untreated (control) and from chronic DEA treated dog hearts, respectively. The onset kinetics of I_{CaL} block elicited by chronic DEA administration are shown in panel **B** (bottom) recorded with 500 ms pulsing cycle length (n=10 dogs for control group and n=7 dogs for DEA group, average of 1 – 3 cells for each dog). The "n" numbers refer to the number of dogs, data are expressed as means ± SEM.

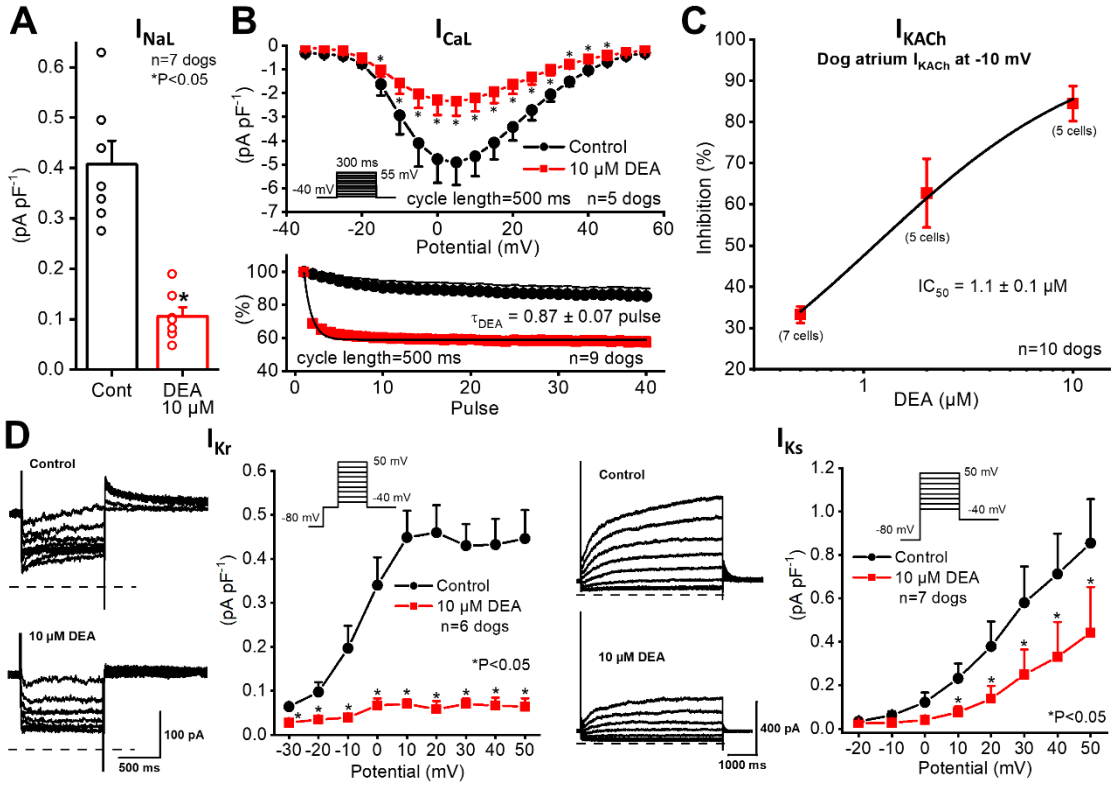

Figure 5. Effect of acute administration of DEA on various transmembrane ion currents. Panel **A** shows the effect of acute DEA administration on I_{NaL} current in dog ventricular myocytes (n=7 dogs, average of 1 – 5 cells for each dog). Open circles indicate individual data points for each dog. Panel **B** shows the effects of 10 μM DEA on the current-voltage relationship of I_{CaL} (n=5 dogs, average of 1 – 3 cells for each dog) and the onset kinetics of I_{CaL} block (n=9 dogs, average of 1 – 3 cells for each dog) elicited by 10 μM DEA administration recorded in left ventricular myocytes, respectively. In these measurements the pulsing cycle length was 500 ms. Panel **C** shows the effect of acute DEA application on I_{KACh}. Concentration-response curves measured at -10 mV indicates IC_{50} values of 1.1 μM. In panel **D** the effects of acute DEA administration on the rapid (*left*, n=6 dogs, average of 1 – 3 cells for each dog) and slow (*right*, n=7 dogs, average of 1 – 3 cells for each dog) delayed

rectifier potassium (tail) currents in dog ventricular myocytes are shown. The “n” numbers refer to the number of dogs, data are expressed as means ± SEM.

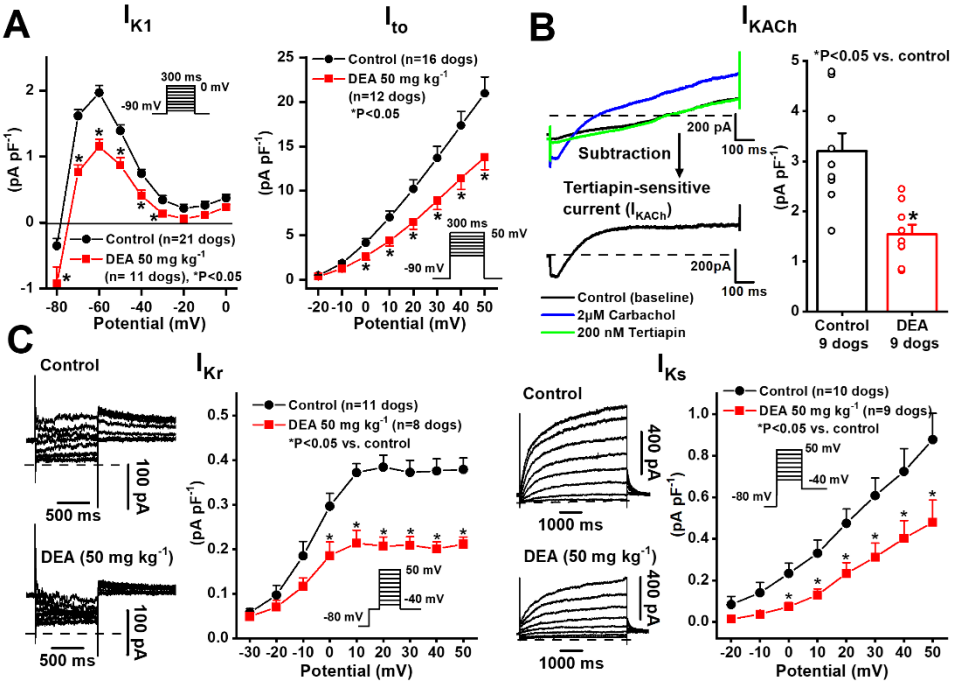

Figure 6. Effects of chronic DEA administration on the outward potassium currents. Panel **A** shows the effect of chronic DEA treatment on the inward rectifier potassium current (*left*, n=21 dogs for control group and n=11 dogs for DEA group, average of 1 – 12 cells for each dog) and on the transient outward potassium current (*right*, n=16 dogs for control group and n=12 dogs for DEA group, average of 1 – 12 cells for each dog) in dog ventricular myocytes. Panel **B** indicates original current traces for I_{KACh} measurements recorded from dog atrial myocytes. The I_{KACh} current was activated by 2 μM carbachol. At the end of the experiments 200 nM tertiapin was applied, which completely and selectively blocked the current. The I_{KACh} was defined as tertiapin sensitive current. On the right bar diagram indicates the density of I_{KACh} at -10 mV in myocytes isolated from untreated (control) and chronic DEA treated dog hearts (n=9 dogs for control group and n=9 dogs for DEA group, average of 1 – 3 cells for each dog). Open circles show individual data points for each dog. In panel **C** the effects of chronic DEA administration on the rapid (*left*, n=11 dogs

for control group and n=8 dogs for DEA group, average of 1 – 6 cells for each dog) and slow (*right*, n=10 dogs for control group and n=9 dogs for DEA group, average of 1 – 7 cells for each dog) delayed rectifier potassium (tail) currents in dog ventricular myocytes are shown. The "n" numbers refer to the number of dogs, data are expressed as means ± SEM.

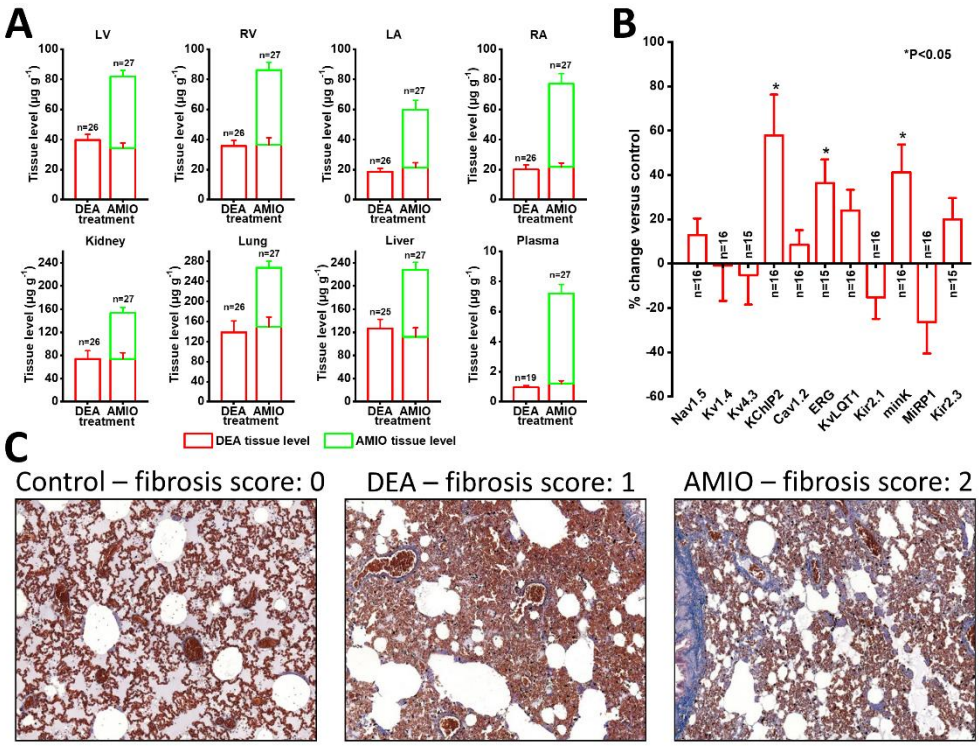

Figure 7. DEA and AMIO tissue levels and the effect of chronic DEA treatment on the mRNA expression levels of various ion channel subunits. Bar diagrams on panel **A** show DEA and AMIO tissue levels in left ventricle (LV), right ventricle (RV), left atrium (LA), right atrium (RA) and in kidney, lung, liver, plasma in DEA and AMIO treated (50 mg kg^{-1}) dogs (n=26 dogs for DEA group – except liver n=25 and plasma n=19 – and n=27 dogs for AMIO group). Panel **B** indicates the changes of expression levels of mRNA of various ion channel subunits after chronic DEA administration. The "n" numbers refer to the number of dogs where tissue samples were obtained from. Panel **C** shows representative histological slides of pulmonary tissue for connective tissue visualization using Crossmon's trichrome staining from the control, chronic DEA treated (25 mg kg^{-1} day^{-1}) and AMIO treated (25 mg kg^{-1} day^{-1}) dogs.

Table 1. The effect of chronic 4 weeks oral treatment of Desethylamiodarone and Amiodarone on ECG parameters in conscious dogs with the corresponding plasma and heart drug concentrations.

	DESETHYLAMIODARONE 25 mg kg^{-1} day^{-1} pro 4 weeks n=11		**DESETHYLAMIODARONE 2 x 25 mg kg^{-1} day^{-1} pro 4 weeks n=27**		**AMIODARONE 2 x 25 mg kg^{-1} day^{-1} pro 4 weeks n=27**	
ECG	**CONTROL**	**DEA**	**CONTROL**	**DEA**	**CONTROL**	**AMIO**
PP interval	596.3 ± 28.0	675.8 ±	573.6 ± 20.7	***685.6 ±***	552.1 ±13.3	***777.7***
PQ interval	103.6 ± 2.1	103.2 ±	102.0 ± 2.1	***110.2 ± 2.5***	99.0 ± 2.5	***118.8***
QRS interval	44.8 ± 2.7	49.1 ±	36.1 ± 0.9	***39.3 ± 1.1***	43.6 ± 2.1	***47.4***
QT interval	208.4 ± 5.1	***238.7 ±***	197.3 ± 3.3	***227.6 ± 3.1***	196.5 ± 2.4	***243.9***
QT_c interval	243.6 ± 3.3	***266.9 ±***	230.8 ± 2.4	***252.2 ± 3.3***	235.5 ± 2.1	***263.3***
Tissue concentration	**DEA**		**DEA**		**AMIO**	**DEA**
Left atria	7.0 ± 1.6		18.4 ± 2.4 (n=26)		38.5 ± 6.2	21.3
Right atria	7.3 ± 1.6		20.1 ± 3.0 (n=26)		55.4 ± 6.8	21.6 ±
Left ventricle	17.3 ± 3.7		39.7 ± 3.7 (n=26)		47.4 ± 4.1	34.4 ±
Right	15.2 ± 3.7		35.6 ± 3.8 (n=26)		49.7 ± 5.3	36.4 ±
Plasma	0.29 ± 0.05		0.96 ± 0.11 (n=19)		6.0 ± 0.6	1.2 ±

P < 0.05 versus Control

Table 2. The effect of chronic DEA treatment on the major action potential parameters

Parameters	Atrial muscle CL=500 ms		Ventricular muscle CL=1000 ms		Purkinje fiber CL=500 ms	
	Control (n=24 dog)	DEA (n=14 dog)	Control (n=29 dog)	DEA (n=24 dog)	Control (n=15 dog)	DEA (n=13 dog)
RP (mV)	-86.1 ± 1.4	***-80.9 ± 1.9***	-88.3 ± 0.8	-89.3 ± 0.6	-91.6 ± 0.6	***-87.7 ± 0.9***
APA (mV)	102.1 ± 2.2	***92.8 ± 1.9***	110.1 ± 1.3	***106.0 ± 0.8***	126.1 ± 1.5	***118.0 ± 2.5***
V_{max} ($V\ s^{-1}$)	254.2 ± 18.8	***165.9 ± 10.7***	213.9 ± 8.8	***164.3 ± 8.0***	487.1 ± 44.8	443.2 ± 23.7
APD_{50} (ms)	60.7 ± 2.7	67.3 ± 3.9	172.4 ± 3.0	***193.1 ± 5.2***	151.1 ± 8.3	138.6 ± 6.3
APD_{90} (ms)	129.3 ± 3.3	***149.3 ± 6.2***	209.9 ± 3.1	***235.3 ± 4.7***	207.3 ± 7.6	213.6 ± 3.0

P < 0.05 versus Control

CL stimulation cycle length, RP resting membrane potential, APA action potential amplitude, V_{max} maximum upstroke velocity, APD_{50} and APD_{90} action potential duration measured at 50% and 90% of repolarization

Table 3. The major pharmacokinetical parameters of DEA and AMIO

		INTRAVENOUS single 25 mg kg^{-1} AMIO or DEA intravenously		**ORAL single 25 mg kg^{-1} AMIO or DEA orally**	
Parameters	Units	AMIO ***DEA (metabolite)***	DEA	AMIO ***DEA***	DEA
$t_{1/2}$ ±SD	h	7.5 ± 1.9 ***3.74 ± 2.85***	10.7 ± 4.1	6.55 ± 2.35 ***6.6 ± 4.2***	10.2 ± 5.1
T_{max} median	h	0.0833 ***0.333***	0.0833	2.5 ***3***	3.0
C_{max} ±SD	µg/ml	79.0 ± 26.7 ***1.68 ± 0.68***	11.5 ± 6.3	1.7 ± 1.3 ***0.23 ± 0.19***	0.52 ± 0.19
AUC_{last} ±SD	µg×h/ml	36.5 ± 9.8 ***5.62 ± 2.4***	8.0 ± 1.8	11.6 ± 7.3 ***1.76 ± 1.10***	4.6 ± 2.4
AUC_{inf} ±SD	µg×h/ml	37.4 ± 9.92 ***5.99 ± 2.64***	9.37 ± 3.22	12.2 ±7.24 ***2.25 ± 1.11***	5.72 ± 2.62
Cl ±SD	ml/h/kg	706 ± 170	2950 ± 1050		
V_{ss} ±SD	l/kg	4.4 ± 1.9	34.9 ± 10.2		
T_{lag} median	h			0 ***1***	0.75
F ±SD	%			35.7 ± 23.7	67.8 ± 48.1
$R_{D/A}$ ±SD	%	15.6 ± 3.5		20.1 ± 10.1	

Parameters regarding DEA after AMIO administration

$t_{1/2}$ apparent terminal elimination half-life, T_{max} time of maximum observed plasma concentration, C_{max} maximum plasma concentration,

AUC area under the plasma concentration-time curve, Cl total clearance, V_{ss} apparent steady-state volume of distribution,

T_{lag} absorption lag time, F bioavailability, $R_{D/A}$ metabolite/parent (DEA/AMIO) ratio